Can long-term fertilization accelerate pedogenesis? Depicting soil processes boosted by annual NPK-inputs since 1928 on bare loess Luvisol (INRAE-Versailles)

Folkert van Oort, Remigio Paradelo, Denis Baize, Claire Chenu, Ghislaine Delarue, Annie Guérin, Nicolas Proix

Can long-term fertilization accelerate pedogenesis? Depicting soil processes boosted by annual NPK-inputs since 1928 on bare loess Luvisol (INRAE-Versailles)

Folkert van Oort[1*], Remigio Paradelo[2], Denis Baize[3], Claire Chenu[4], Ghislaine Delarue[1], Annie Guérin[5], Nicolas Proix[5]

[1] Université Paris-Saclay, INRAE, AgroParisTech, UMR 1402 ECOSYS, 78026 Versailles Cedex, France; folkert.van-oort@inrae.fr; ghislaine.delarue@inrae.fr

[2] CRETUS, Departamento de Edafoloxía e Química Agrícola, Universidade de Santiago de Compostela, 15782 Santiago de Compostela, Spain; remigio.paradelo.nunez@usc.es

[3] INRAE, UR 0272 Science du Sol, 45075 Orléans Cedex 2, France ; denis.baize@inrae.fr

[4] Université Paris-Saclay, INRAE, AgroParisTech, UMR 1402 ECOSYS, 78850 Thiverval-Grignon, France; claire.chenu@inrae.fr

[5] US 0010 Laboratoire d'Analyses des Sols (LAS), 62000 Arras, France; annie.guerin@inrae.fr; nicolas.proix@inrae.fr

Abstract. Human activities worldwide menace beneficial soil ecosystem services, but long-term anthropogenic impacts on soil properties and processes are often difficult to assess in field conditions. Here we exploited INRAE's patrimonial '42-plots' bare-fallow experiment, an unique long term experiment in the world created in 1928 in Versailles (France), to emphasize long-term impacts of annual inputs of NPK fertilizers (ammonium, phosphate, potassium salts) and basic amendments (lime, basic slag) on loess Luvisols. We selected plots receiving monovalent (Na^+, K^+), acid (NH_4^+), basic (Ca^{2+}) and non-amended (reference) plots, thus embracing the today widely diverging physicochemical surface soils conditions. Temporal changes of soil characteristics were studied on historical archived topsoil samples, whereas soil-depth impacts were studied on samples from subsurface horizons collected in 2015 until 120-cm depth. Bare-fallow management caused a rapid

organic matter (OM) decay, soil acidification, CEC reduction and lixiviation of cations. With reduced OM-buffering capacities, specific fertilizer-induced physicochemical conditions enhanced the development of several soil-forming processes. NH_4-fertilizers amplified soil acidification (pH < 4), lixiviation (*i.e*. 1.5 kg m^{-2} of Ca), aluminization of the exchange complex, and weathering of ferromagnesian minerals and plagioclase feldspars. Under $(NH_4)_2HPO_4$ fertilization, a quasi-total dissolution of chlorite and hornblende occurred, pointing to an acidocomplexolysis process in which the PO_4^{3-} anion likely plays the role of complexing organic acids in Podzols. Ammonium fertilizers also affected E, B and C horizons. In reference plots, similar but lower effects remained restricted to the surface horizon. Na/K-fertilizers favoured substantial clay translocation (*i.e*. 10-15 kg m^{-2}) from the Ap to underlying E and E/Bt horizons. Liming amendments counteracted acidifying effects of OM-depletion, and raised the pH to 8-8.5 and exchangeable Ca to > 95 %. It may be clear that the initial design specifications do not allow a direct comparison with current conditions of agricultural soils. However, in the view of global climate change, foreseeing a lowering of organic carbon contents in soils, the 42-plots trial acts like an "alert launcher", forecasting risks of soil degradation with respect to mineral soil phases, parameters and processes, generally buffered and masked by the presence of organic matter. The 42-plots experiment forms a high-valued playing field for experimental research, offering a unique centennial time-span of differing physicochemical properties in a soil context with close initial pedogenetic connexion.

Keywords: long-term bare-fallow experiment; fertilization; loess soil; clay leaching; acidification; mineral weathering

*Corresponding author

Highlights

- 85 years fertilization forced soil forming processes in a bare-fallow loess Luvisol
- ammonium fertilizers promoted acidification, aluminization and mineral weathering
- $(NH_4)_2HPO_4$ caused acidocomplexolysis and loss of primary ferromagnesian minerals

- clay leaching was amplified under prolonged inputs of Na- and K-based fertilizers
- top horizon of non-amended reference plots showed notable pedogeochemical changes

1. INTRODUCTION

Worldwide, agricultural intensification during the second half of the 20th century led to decreasing organic matter (OM) contents and soil structure stability and to growing risks of soil erosion (Montanarella, 2010; Lal, 2015). In northern France, loess soils are widely used for intensive cereal cropping, but they are sensitive to acidification, loss of SOM, and erosion (Bresson and Boiffin, 1990; Le Bissonnais *et al.*, 1996; Arrouays et al., 2002; Gis Sol, 2011). Anthropogenic pressure represents major threats for sustainable land use and soil ecosystem services. Therefore, it is urgent to identify, understand and anticipate the risks of soil degradation caused by human activities (Lal, 2015).

Recurring application of mineral fertilizers and amendments is increasingly questioned with regard to potentially harmful impacts on physical, chemical and biological soil properties (Haney, 2017), as well as their role as a source for micropollutants (*i.e.* Kabata-Pendias, 2011; van Oort et al., 2017a). One main effect of mineral fertilizers on soil properties lies in the input of dominant cations, either as target (K^+, Ca^{2+}, Mg^{2+}) or accompanying elements (Na^+, H^+). By deeply modifying the cation composition of the soil's exchange complex, fertilizers may significantly change soil properties and processes (van Breemen and Buurman, 2013), particularly in soils with low SOM contents (Paradelo *et al.*, 2016). Thereby, ammonium fertilizers introduce substantial amounts of protons, causing soil acidification and formation of protonated hydrogen clay. Such H-saturated clays are unstable since protons enter the octahedral layer and free large amount of aluminium, and evolve rapidly into Al-saturated clay, finally leading to clay destruction (Eeckman and Laudelout, 1961; Bolt and Bruggenwert, 1976). With time, the prolonged use of ammonium fertilizers generate large amounts of exchangeable Al on the exchange complex (Sposito, 1989), highly toxic for plants. Monovalent Na, and to a lesser extend K fertilizers promote clay dispersion and leaching, leading to soil densification and periodically water logging (Levy and Torrento, 1995; Sparks, 2003; Paradelo et al. 2013). Intensive soil liming by adding basic amendments may lead to high amounts of exchangeable Ca,

unbalancing the soil's Ca/Mg ratios and Fe availability, inducing chlorosis in plants due to iron deficiency (Filipek, 2011). In field conditions however, the effects of long-term fertilization are often difficult to assess due to varying soil nature, land use and lacking historical information on fertilizer input management.

Long-term agricultural experiments offer unique opportunities to study the cumulative effects of fertilizers and amendments on crops and soils. Many historical experiments initiated since the middle of the 19th century, primarily focusing on the benefits of fertilization on increasing crop production and quality: *i.e.* Rothamsted, England (1843); Sachsen, Germany (1851); Gembloux, Belgium (1872); Grignon, France (1875); Urbana-Illinois, United States (1876); Wageningen, The Netherlands (1877); Askov, Denmark (1894). However, little attention was paid at that time to potential negative impacts of chemical fertilizers on soil composition and properties. Therefore, when at the end of World-War 1, broad need raised for reviving the French agriculture, notably by introducing a massive use of chemical fertilizers, a long-term bare fallow (LTBF) experiment was initiated in Versailles in 1928: the 42-plots trial giving special attention to the mineral soil fraction. Its initial objectives were to "*examine the impacts of prolonged applications of main N, P and K-fertilizers, as well as organic and basic amendments on the composition and properties of loam soils*" (Burgevin and Hénin, 1939). The experiment was established on silt-loam textured loess soils, representative of large areas under conventional cereal production in northern France and NW Europe, and under bare fallow management (no vegetation, no cultivation). With its historical archive of soil samples, collected since March 1929, the 42-plots trial is currently the oldest bare-fallow field experiment in the world. Bare soil management was presumed to exacerbate the impacts of fertilizers on the soil (Burgevin and Hénin, 1939). Although not virtually reflecting real field conditions of agricultural soils, bare-fallow trials represent a playground for experimental pedology under local climatic conditions, offering exceptional opportunities to unravel long-term aspects of intensive fertilization impacts on soil ecosystem services. Thus, the 42-plots trial gives access to the speed, chronology and limits of

soil processes that either may develop or amplify under long-term fertilization practices and corollary contrasting physicochemical conditions, offering an exceptional, centenary, retrospective view. It represents a valuable tool to answer questions whether chemical fertilizers can influence soil formation at a centenary time-span.

The present work assesses both temporal and soil-depth-impacts on major soil parameters, organic carbon and clay contents, soil pH and cation exchange complex, in a bare-fallow Loess Luvisol, constrained by almost 90 years of fertilization. Based on exhaustive previous pedogeochemical work (van Oort *et al.*, 2016, 2017a, 2018, 2020a,b), we selected a series of treatments of nitrogen, phosphorus and potassium fertilizers as well as basic amendments and non-amended reference plot, representative for current contrasting physicochemical properties in the soils of the experiment. For each treatment, we analysed surface samples from the historical collection and compared them with analyses from subsurface E, Bt and C horizons, collected in 2015. The aims were to depict the extent of differentiation of the main soil physicochemical properties during almost 9 decades in the surface horizon, and to assess the magnitude and depth of impacts in subsurface horizons. Considering the great number and wide panel of results, we employed a close '*Results-Discussion*' canvas, linking inputs of fertilizers to effects in terms of accelerated soil forming processes and pedogenesis.

***NB**. Limited amounts of historical samples can be provided on demand, for original complementary research* (folkert.van-oort@inrae.fr).

2. MATERIALS AND METHODS

2.1 Experimental design

The LTBF experiment of INRAE started in 1928 in the gardens of the Versailles Chateau on *in-situ*, silt loam textured Haplic Luvisol (IUSS, 2014), developed in Late Weichselian calcareous loess

(Antoine et al., 2003), initially containing 15-25% $CaCO_3$. The experiment included 42 plots of 2 × 2.5 m within a total surface of 200 m², a small area with a flat topography where limited edaphic and geological heterogeneity is expected, thus favouring an initially close pedogenetic connection between soils of each plot, with respect to soil nature, behaviour, and physical and geochemical properties. Of course, this does not preclude some local variability of rapidly changing parameters such as the soil organic matter contents and related exchange properties. Since the start, the experimental design remained unchanged for more than 90 years. Sixteen fertilization treatments were manually applied at the soil's surface, in duplicate, and incorporated in the 0-25-cm soil layer. Equivalent NPK-inputs per ha/year are shown in Table 1. Ten reference plots without inputs complete the 42-plots trial. The plots were kept free from weeds and the surface layer was turned-over by hand twice a year, in spring and autumn, to a depth of 25 cm. Samples have been collected annually in the 0-25-cm-layer, nowadays every three to five years, air-dried, ground, sieved at 2 mm and stored in the dark at room temperature. Five samples were taken in each plots, homogenized and then about 800 g were stored. The soil archive currently includes ≈ 3000 bare-soil surface samples, covering more than 9 decades, a world's unique collection (Figure 1).

2.2 Sample selection

For the study of temporal changes of soil parameters, series of about 15 historical samples were analysed for the 1929–2014 period with an average interval of 6 years, closer during the first decades (3 years) where changes were supposed to happen faster, and more spaced in recent decades. The first samples in the collection are from March 1929, i.e. 5 months after the start of the experiment in November 1928 (Burgevin and Hénin, 1939). We selected different treatments accounting for major contrasting physicochemical surface soil conditions, following previous detailed pedogeochemical inventory work (van Oort *et al.*, 2016, 2017a), in order to examine the principal fertilization-induced soil processes. Our plot selection included two types of fertilizers with acidifying effects (ammonium sulphate, ammonium phosphate), three types of fertilizers with clay-dispersive effects (sodium

nitrate, sylvinite, potassium chloride), two types of amendments with pH-increasing effects (basic slag, calcium carbonate), as well as two non-amended reference plots (Table 2). In the same selected plots, additional sampling was performed in 2015 in subsurface horizons to 120 cm soil depth, using a root auger device (∅ 8cm, h 15 cm, Eijkelkamp, Giesbeek, The Netherlands). The core samples were separated according to soil horizon limits. Selected undisturbed parts were air-dried and resin-impregnated for thin-section preparation; the rest was ground, sieved to < 2 mm and stored for chemical analyses.

2.3 Analyses

Analyses were performed according international standard protocols at INRAE's National Soil Analysis Laboratory (LAS): pH in water (NF ISO 10390), grain size distribution (NF X 31-107), organic carbon (NF ISO 10694) and nitrogen (NF ISO 13878). The cation exchange capacity (CEC) and exchangeable cations was using the hexamminecobalt trichloride extraction method (NF ISO 23470), noted noted CEC_{Cohex}.), working at low concentrations, close to *in situ* soil field conditions (Ciesielski and Sterckeman, 1997a,b). This reagent limits the development of additional variable charge exchange sites with respect to methods using buffered solutions (e.g. ammonium acetate at pH 7, Metson) and the release of elements from non-exchangeable sources (Ca from carbonates in alkaline conditions, Al from aluminium oxyhydroxydes in acidic conditions, K from lattice positions). For the 42-plots trial, Pernes-Debuyser and Tessier (2002) modelled the differences between Cohex and Metson as a function of soil pH. These authors showed that in 1999 the Cohex data for acid and alkaline treatments varied from single to double (6.9-13.6 $cmol^+ kg^{-1}$), whereas they differed less than 15 % when using the Metson method. Moreover, they highlighted a minimum CEC_{Cohex} value of 8 $cmol^+ kg^{-1}$, accredited to the intrinsic permanent charge of the mineral clay fraction for 1 kg of soil.

Selected undisturbed parts of the centre of core samples were transferred into hard cardboard boxes (7.5 cm × 7.5 cm × 4 cm), air-dried and impregnated with polyester resin, before cutting and

polishing to 30-µm thickness for the production of thin sections (FitzPatrick, 1993). The nature, morphology and organization of coarse soil constituents and the fine plasma were studied with a petrographic Nikon Eclipse E400 polarizing light microscope, using the terminology currently employed in soil micromorphology (Stoops, 2003).

The silty-loam textured Luvisol contained about 40% of coarse silt (20-50 µm) and 20% of fine silt (2-20 µm). The latter fraction includes the main part of weatherable primary minerals whose weatherability increases with decreasing particle size (van Oort, 2018). Consequently, impacts of infra-centennial fertilization practices on the soil's solid phase will be visible first on fine silt fractions. Hence, after preliminary standard granulometric extractions of clay, fine and coarse silt and sand fractions, we separated the 2-20-µm fine-silt fraction into 2-5 µm, 5-10 µm, and 10-20 µm subfractions by exhaustive repetitive sedimentation extractions in glass cylinders. X-ray diffraction (XRD) diagrams were made on oriented deposits of fine silt subfraction suspensions (25 mg/ mL) with a Siemens D-5000 Kristalloflex diffractometer (Co K*α* radiation, 30 mA, 40 kV). Total element concentrations were determined at LAS on fine silt subfractions after tri-acid (HF, HNO_3, $HClO_4$) digestion (ISO NF X31-147) for Ca, K, Mg, Na, Al, Fe, and scandium (Sc) by ICP-AES spectrometry (NF ISO 22036).

2.4 Data presentation and statistics

Results of temporal and soil-depth changes of major soil parameters, sensitive to anthropogenic pressure on soils (organic carbon contents, pH, CEC, clay contents) are simultaneously presented for each selected fertilization treatment. For the reference plots, we presented average values and max/min bars. Specific marks used to identify different treatments are detailed in Table 2. Soil-depth concentration profiles were compiled using data from surface horizons sampled in 2014, and from subsurface horizons sampled in 2015.

ANOVA was used to assess the influence of treatment on the main soil properties (pH, OC, CEC, clay content, Table 3). The homogeneity of variance was tested using the Levene test and the

normality of data was checked using the Shapiro-Wilk test. When a significant effect of land use at a level of significance of $P<0.05$ was found, the Tukey's multiple range test was used to separate groups. Data that did not pass the normality test were log-transformed for ANOVA. All statistical analyses were performed using the R statistical package for MacOSX version R 3.1.3 (R Core Team, 2019) and the package R Commander version 2.6-1 (Fox and Bouchet-Valat, 2019).

3. Results & Discussion

3.1 Physicochemical properties

3.1.1 Organic carbon

After its use as extensive grassland, the organic carbon contents in the surface horizon decreased rapidly under bare fallow management (Figure 2a), first by about 30% from 14-18 g kg^{-1} to 10-12 g kg^{-1} in only one decade (1929-1940), then more progressively reaching a content of 4-6 g kg^{-1} in 2008. Initial variability of OM contents during the first years of the experiments express a typical divergence related to previous land use. The data from 2014 showed slightly increasing discrepancy between the organic C data, for unknown reasons. Today, the organic matter (OM) pool is quasi-exclusively formed by persistent organic carbon, with a plural centennial residence time, and intimately bound to the mineral fraction (Barré et al., 2010). More details on OM dynamics and modelling on 42-plots historical samples, can be found in Barré et al. (2010, 2016, 2018), Lefèvre et al. (2014), Menichetti et al. (2015), Paradelo et al. (2013, 2016), Lutfalla et al. (2017), and Cécillon et al. (2018).

Bare fallow conditions lead to OM depletion in all treatments (except for horse manure plots). Since the last four decades (Table 3, Figure 2a), diverging trends of OM contents emerged: for acid and basic treatments, OC contents were higher than those of the reference plots, whereas for the monovalent treatments, they were either fairly similar ($NaNO_3$ plot) or noticeably lower (potassium

fertilizers, sylvinite, KCl). Concordant findings were reported by Paradelo et al. (2016) who examined the relation between physical protection of organic matter and aggregate stability in surface samples of KCl, $CaCO_3$ and reference plots. Such diverging tendencies illustrate the driving control of a marked physicochemical ambiance on soil OM (Kögel-Knabner and Kleber, 2011). Usually, the role of Ca^{2+} is well recognized for its stabilizing effect on OM (e.g. Six et al., 2004; Wuddivira and Camps-Roach, 2006; Paradelo et al., 2015; Rowley et al, 2018). In acid soils of temperate regions, and in many tropical volcanic soils, the stabilizing role of Al^{3+} was ascribed to the formation of Al-hydroxyl complexes with OM (e.g. Scheel et al., 2008; Heckman et al., 2013; Takahashi and Dahlgren, 2016). Monovalent Na^+ and K^+ produce a clay dispersive effect, leading to soil structure degradation and an enhanced accessibility of microorganisms to OM (Levy and Torrento, 1995; Paradelo et al., 2013, 2016). The lowest OC contents were observed under K-fertilizers. Such different behaviour toward OM dynamics of K^+ with respect to Na^+ may be ascribed to smectite-illite transformation by K-retrogradation (Pernes-Debuyser et al., 2003), lowering the clays reactivity, specific surface and exchange capacity (Andreoli, 1989; Andreoli et al., 1989), thus easing the decomplexation of OM.

Effects of centennial OM depletion in this experiment were mainly restricted to the surface horizon. In subsurface horizons (Figure 2b), the organic C content profiles showed little divergence between the treatments: below the E/Bt horizon, the range of variation between the different treatments was reduced to ≈ 1 g kg^{-1}, and total organic C content decreased from ≈ 3 to ≈ 1 g kg^{-1} in the calcareous loess.

This short overview emphasised the high-added value of the 42-plots LTBF experiment for unravelling complex mineral-organic associations that prevail in different pedogenetic environments (Kleber et al., 2015; Kögel-Knabner and Amelung, 2021). It offers indeed an exceptional historical sample set covering 92-years of OM decomposition, in a soil context with currently wide varying physicochemical conditions, but initially close pedogenetic connexion.

3.1.2 Soil pH

With time, pH ranges in the surface horizons significantly differed between the acid, basic and monovalent Na/K and reference treatments (Table 3). For the reference plots and monovalent treatments, the pH dropped by about 1 unit during the first 10 to 15 years (Figure 2c), for a great part due to decomposing OM: CH_2O (OM) + O_2 → CO_2 + H_2O → HCO_3^- + H^+ (Bolt and Bruggenwert, 1976). Since the 1940's, the pH in the reference plots stabilized around 5 (4.7-5.4); under potassium fertilizers (KCl), the pH remained fairly close to those in the reference plots (Figure 2c), whereas sodium-based fertilization ($NaNO_3$) caused a slight pH increase with time, to 6.7-6.8. The input of a mixed Na-K fertilizer (sylvinite) led to pH values intermediate between the pure K and Na treatments. Ammonium fertilizers exert strong acidifying effects on soils (Bouman et al., 1995), due to the production of protons by nitrification: $NH_4^+ + 2O_2 \rightarrow NO_3^- + 2H^+ H_2O$. Thus, di-ammonium phosphate $(NH_4)_2HPO_4$ introduces one more proton with respect to ammonium sulphate $(NH_4)_2SO_4$. Between 1929 and 1940, the pH in the ammonium fertilizer treatments dropped by about two units from 6.4 in 1928 (Burgevin and Hénin, 1939) to 4.4-4.6 today, as a conjugated result from nitrification and OM decomposition. These data were close to pH determinations reported as soon as 1939 (Burgevin and Hénin, 1939). A "plateau-value" around pH 4 occurred between ≈ 1960 and 2000, but since, a new pH decrease was noted for the ammonium treatments, currently around pH 3.5. Such stepwise pH decrease pointed to a changed soil acid neutralizing capacity (van Breemen et al., 1983), announcing the alteration of soil constituents. For the basic amendments, the pH rapidly increased during the two first decades of the experiment, in spite of the acidity produced by OM decomposition. The rate of increase was higher for $CaCO_3$ than for basic slag. Since the 1950's, the pH continued to increase more progressively, reaching currently 8.2-8.5. For both treatments, about 2 % of calcium carbonate was found in the surface horizon in 2014 (van Oort et al., 2016).

In subsurface horizons of reference plots and K-based treatments, the soil pH evolved quite similarly, increasing gradually from pH 6 in the E horizon, to pH ≈ 7 in the E/Bt or upper Bt horizons and reaching pH 8 in the carbonate-rich Ck horizon (Figure 2d). Nevertheless, such pH-depth profiles

suggested a moderate acidification of the upper 50 to 60 cm, when comparing them with pH gradients in similar, nearby, soils under cultivation with pH > 7, down from the plough layer (Isambert, 1979; Moni, 2008). The Na-based fertilizers demonstrated such a pH-depth profile with pH > 7. As to the long-term input of NH_4-fertilizers, they strongly marked the soil with pH values by 1.5 to 3 units lower than observed for the reference plots, until the calcareous loess parent material (Figure 2d). In the NH_4-sulfate plot, the pH was < 4 in the upper 60 cm, and < 4.5 in the Bt horizon, but under NH_4-phosphate, the acidifying impacts diminished earlier in the soil profile, reaching pH ≈ 6 in the Bt horizon. Basic amendments had an opposite effect, with pH ≥ 8 in all soil horizons.

3.1.3 Clay contents

Temporal evolution of clay contents was determined for 9 sampling periods for each series of samples (Figure 3a). During the first decades of the experiment, the interval of clay contents remained rather low, between 15-20 g kg^{-1} for all treatments. However, as organic matter depletion proceeds, specific effects of contrasting cation compositions on clay dispersion/aggregation (Talibudeen, 1981) become more clearly expressed. Thus, in the Na and K treatments, clay contents decreased more rapidly than observed in the reference plots (Table 3) and are clearly lowest since the 1990s (130-150 g kg^{-1}) with respect to all other treatments. Such low contents point to a process of dispersion and leaching of clay from the surface to subsurface horizons, favoured by Na and K salts (Wilding and Tessier, 1988; Tessier, 1990). For the 42-plots experiment, clay losses between 1929 and 2014 from the 0-25-cm Ap horizon were estimated at ≈ 15 kg m^{-2} for Na-based fertilization and at ≈ 8 kg m^{-2} under K-fertilizers (van Oort et al., 2018). Surprisingly, in the acid treatments, clay contents in the surface horizon tend to increase in comparison to reference plots, particularly since the end of the 1990s. More detailed clay extraction studies are needed to confirm such tendency. Increasing clay contents with time under strong acidic conditions was previously hypothesized to result from the weathering of silt-sized primary minerals (van Oort et al., 2016). Such hypothesis was supported by positive geochemical budgets of clay-constitutive or clay-associated major (Fe, Al) and

minor (Sc, Tl, As) elements in the surface horizon of ammonium fertilizer plots between 1929 and 2014 (van Oort et al., 2018). Such effect was stronger for ammonium phosphate than for ammonium sulphate.

At depth, clay contents in E horizons were highest for Na and K fertilizers (Figure 3b). Strong clay gradients between Ap and E horizons argue for contemporary clay illuviation process, directly under the Ap horizon. At greater depth, clay contents under $NaNO_3$ inputs were clearly higher than for the other treatments, stressing the role of sodium for amplifying clay illuviation.

3.1.4 Cation exchange capacity

In the reference plots, the CEC_{Cohex} decreased steadily between 1929 and 2014 (Figure 3c) as the result of a twofold mechanism: a net loss of exchange sites due to OM decomposition, and a loss of variable negative charges on organic and mineral components, neutralized by H^+ produced from decaying OM (Bolt and Bruggenwert, 1976; Julien and Turpin, 1999). The CEC_{Cohex} values in soils under ammonium-based fertilization decreased more rapidly than in the reference plots between 1929 and the early 1940's. Obviously, the additional input of protons by nitrification of ammonium resulted in a rapid lowering of soil variable charges (Kunhikrishnan et al., 2016).

In monovalent Na/K treatments, the CEC_{Cohex} also rapidly decreased during the first decade of the experiment, which can be attributed to the conjugated effects of disaggregation, enhancing and OM mineralization and possibly favouring clay leaching. As shown in Figure 2a, the organic carbon contents are lowest for the Na/K treatments as soon as the first decades of the experiment. Besides, a marked soil structure degradation and decreased macroporosity for in the surface horizon for soils under Na and K-fertilizers were already noted at the end of the first 10 years of experiment (Burgevin and Hénin, 1939). For both acid and monovalent Na/K treatments, the CEC_{Cohex} decrease lessened and values remained between approximately 7 and 9 $cmol^+ kg^{-1}$, close to the estimated permanent charge of 8 $cmol^+ kg^{-1}$ (Pernes-Debuyser and Tessier, 2002). Such plateau level was more pronounced for ammonium sulphate than for di-ammonium phosphate, and lower for K than for Na treatments.

Moreover, since the 1950's, CEC_{Cohex} data under inputs of $(NH_4)_2HPO_4$ are obviously lower than in the case of $(NH_4)_2SO_4$. A receivable explanation refers to the formation of aluminium phosphates in acid soil conditions and their great affinity for clay surfaces (Sposito, 1989). Thus, phosphates breaking external OH^- sites would results in lowered net charge (Parfitt, 1978), and preferential adsorption of Al-phosphates on clay particles favours strong aggregation, and reduce clay surface area and accessible exchange sites (Edzwald et al., 1976). In addition, adsorption of hydroxyl-Al in clay interlayer also causes a CEC decrease (Barnhisel and Bertsch, 1989). Since 2000 however, the CEC_{Cohex} for acid and Na/K treatments dropped again, attaining about 5-7 $cmol^+ kg^{-1}$ in 2014. Such low values suggest recent modifications in the mineral soil composition. By contrast, under basic amendments, the CEC_{Cohex} varied little, decreasing from ≈ 16.5 to ≈ 13 in 85 years (Figure 3c). Liming improves soil structure by increasing and strengthening clay-OM bonds (Oades, 1984; Kunhikrishnan et al., 2016), thereby lowering OM accessible to microbial decomposition.

In subsurface horizons, CEC_{Cohex} values in soils under NH_4^+ fertilizers were clearly lower than in the reference plots (Figure 3d), indicating that acidifying soil conditions led to a loss of variable charge to considerable depths. The effect was greater for $(NH_4)_2HPO_4$ than for $(NH_4)_2SO_4$ in the E horizon, but inversed in the Bt horizon, in agreement with a lower pH (6.1 vs. 4.2, resp. Figure 2b). In potassium treatments, CEC_{Cohex} data were lower than in the reference plots, until the Bt horizon, suggesting an effect of K-retrogradation by vermiculite-smectite clay minerals (Pernes-Debuyser et al., 2003; Huang, 2005). Among all treatments, the highest CEC_{Cohex} values in subsurface horizons were observed under Na-based fertilizers, suggesting clay enrichment by enhanced leaching. Under basic amendments, the CEC_{Cohex} were higher than in reference plots, notably in E and E/Bt horizons (Figure 3d). At high pH, the CEC comprise both permanent and variable charges (Julien et Turpin, 1999).

3.1.5 Exchangeable cation compositions

Since 1928, soil acidification in the ammonium treatments produced a virtually perfect inversely proportional replacement of Ca_{exch} by Al_{exch} (Figure 4). Replacement of Ca by Al was more rapid under

NH_4-sulphate (P2) than under NH_4-phosphate (P14) fertilization: at the end of the 1950s, after only 3 decades, the first exhibited already more than 60 % of Al_{exch} versus < 25 % for NH_4-phosphate, but such divergence diminished rapidly since the 1990s.

Today, Al_{exch} occupies ≈ 95-98 % of the cation composition in both treatments. Until the 2000s, Mg_{exch} represented ≈ 10 % for NH_4-sulphate treatment, versus ≈ 20 % for NH_4-phosphate, but its presence strongly decreased in 2014. In reference plots, significant amounts of Al_{exch} appeared in the 1960s as the pH reached ≈ 5; Al_{exch} proportions increased since the 2000s reaching ≈ 20 % in 2014.

Basic amendments (P35, P39) progressively chased all exchangeable cations other than Ca, Ca_{exch} currently occupying 96-98 % of the exchange complex. Long-term input of K-fertilizers progressively increased the proportion of Al_{exch}, up to ≈ 30 % of the CEC for KCl (P23), and to 15-20 % of the CEC for the mixed Na/K fertilizer sylvinite (P29). Under sodium-based fertilization ($NaNO_3$, P4), the proportion of Na_{exch} increased up to 10-20 % of the CEC and little or no Al_{exch} was observed. Remarkable amounts, up to 5 % of the CEC for Mn_{exch}, were detected notably under inputs of ammonium (P2, P14) and under Na-K-fertilizers (P23, P4). For NH_4-treatments, the presence of Mn_{exch} highlighted a process of Mn lixiviation to depth under acid soil conditions; for Na/K-treatments, higher Mn_{exch} amounts were ascribed to clay leaching, aggregate dispersion, soil densification and temporary anaerobic conditions as demonstrated by the typical mottling observed during profile sampling.

At depth, high proportions of exchangeable aluminium in subsurface horizons emphasized the impacts of soil acidification due to repeated inputs of ammonium. For NH_4-sulphate, Al_{exch} exceeded 90 % of the cation composition as deep as the Bt1 horizon (70 cm) and still reached 25 % in the Bt2 horizon until 80 cm depth (Figure 5a). For NH_4-phosphate, high Al_{exch} rates (> 90 %) were observed until 40 cm depth in the upper horizons Ap and E, lowering to ≈ 50 % in E/Bt and to < 5 % in the Bt1 horizon (Figure 5b). Interestingly, in both soils, Mn_{exch} reached maximum values (≈ 5 %) as the pH raised above 4.5 in the Bt2 and E/Bt horizons under ammonium sulphate and -phosphate

respectively, consistent with Mn-lixiviation in strongly acid conditions. Such detection of exchangeable Mn at depth in the acid treatment plots was remarkable, since for all other treatments, the exchangeable Mn contents were generally below the detection limit (< 0.005 $cmol^{+}\ kg^{-1}$). In reference plots, the effects of soil acidification under local climatic conditions remained mainly restricted to the Ap surface horizon, Al_{exch} in the underlying E horizons was < 1% (Figure 5c).

Basic amendments enhanced > 90 % Ca_{exch} saturation of the CEC in all horizons, allowing a maximum of 5-10% of other exchangeable cations to occur, mainly magnesium (Figure 5d,e). Long-term input of K-fertilizers enhanced proportions of K_{exch} up to 10-13 % until the B1 horizon (Figure 5f), but for sylvinite such abundance was hampered by appreciable proportions of Na_{exch} (Figure 5g), occurring as deep as in the carbonated loess at 120-cm depth. Under Na-based fertilizer, about 10 % of Na_{exch} was present in subsurface horizons down to the BC horizon (Figure 5h).

3.2 Soil microstructure and mineralogy

3.2.1 Micromorphology of contemporary pedofeatures

Pedofeatures are discrete soil fabric units recognizable from adjacent groundmass material by a different concentration in one or more components, or by a different internal fabric (Stoops, 2003). They are key indicators for current or past soil forming processes, changing land use or soil management practices (Stoops et al., 2010), as well as for metal pollutant transfer in soils (van Oort et al., 2007, 2017b, 2018). Thus, pedofeatures observed under specific fertilization treatments, demonstrating occurrence, abundance or extension that distinctly differed from other treatments, as well as from pedofeatures issued by local loess Luvisol pedogenesis, attest for contemporaneous fabrics deriving from the 42-plots experimental conditions (Figure 6).

Distinctively under inputs of Na- and K-based fertilization, numerous layered and compound-layered clay-silt coatings were observed covering the surface of large voids in subsurface horizons, with a thickness up to several hundreds of microns (Figure 6a-d). They mainly occurred in E and E/Bt

horizons, between 30 and 50 cm depth, but also in the upper parts of the Bt horizon, although of lesser thickness. Their abundance and extent emphasized the amplitudes of estimations for clay-losses from surface horizons, notably under Na–based fertilization, around 10-15 $kg.m^{-2}$ (10-15$t.ha^{-1}$) in 85 years (van Oort et al., 2018).

In reference plots and under acid ammonium-based fertilization, dark matrix coatings (matrans) build up by a mixture of fine particles with various sizes and compositions (clay, silt, oxides and fine organic matter) frequently occurred close below the plough layer (Figure 6e,f). Such matrans are characteristic for surface horizons of agricultural soils with a low aggregate stability (Stoops et al., 2010). In acid soils, under input of ammonium fertilizers, black precipitates frequently occurred at the surface of large pores (channels, vughs) or in the groundmass nearby pores (Figure 6g-i). Such precipitates primarily contained manganese with minor contents of lead, zinc or nickel, as revealed by micro-X-ray-fluorescence work (van Oort et al., 2018). Under ammonium sulphate, manganese coatings (mangans) were present as deep as 80-85 cm, coinciding with low pH values (4-4.5, Figure 2d). Under di-ammonium phosphate, fine dendritic manganese nodules occurred in the proximity of pores in the E/Bt horizon (pH ≈ 4.5). Such localized Mn-accumulations give evidence for strongly acid conditions enhancing lixiviation of mobile elements.

3.2.2 Mineralogy of fine silt fractions

We assumed that the impacts of infra-centennial fertilization practices would primarily affect low-resistant primary minerals in the finest silt fractions (cf. section 2.3). In order to substantiate the impacts of acidifying ammonium treatments, hypothesized to lead to mineral dissolution, we compared mineralogical compositions of fine silt fractions extracted from the 2014 surface horizon samples of (NH_4)-sulphate, (NH_4)-phosphate, reference and calcium carbonate treatments (Figure 7). Considering its rapid pH increase from the start of the experiment, restraining the evolution of aluminosilicate minerals, we assumed that the $CaCO_3$ treatment might represent a better mineralogy control than the reference plots. X-ray diffraction (XRD) diagrams were made on oriented fine silt

deposits, in order to favour the detection of basal *d*(00ℓ) reflexions of (ferromagnesian)-phyllosilicates, primarily affected in loess soils under acid soil conditions (Hardy et al., 1999) as well as the cleavage plan *d*(110) of ferromagnesian amphiboles (Oberti et al., 2018)

For the basic, reference, and ammonium sulphate treatments, the XRD diagrams of the oriented fine silt (2-20-µm) fractions (Figure 7a) showed distinct basal spacing reflexions for mica (*d*(001), *d*(002)) at 1.0 and 0.5nm, respectively, and for chlorite (*d*(001), *d*(002), *d*(003) and *d*(004)), at 1.41, 0.707, 0.471 and 0.353 nm, respectively. The latter spacings point to a trioctahedral ferromagnesian chlorite structure. Interestingly, the broad 1.4 nm reflexion in the $CaCO_3$ treatment suggested the presence of vermiculite. Its absence in the other treatments suggested a local pedogenetic origin by alteration from biotite/chlorite, but disappearing in the silt fractions in acidified soil conditions. Several *hkl* reflexions at about 16°2θ (0.649, 0.638 nm) and in the range of 25.5-29.0°2θ (0.402, 0.378, 0.365 nm) indicated the occurrence of potassium feldspars and plagioclase (F). Amphibole (*d*(110) at 0.842 nm) was poorly detectable on global 2-20-µm-fractions. Strikingly however, the basal reflexions of chlorite strongly diminished or were absent for the $(NH_4)_2HPO_4$, treatment, highlighting a process of dissolution of ferromagnesian phyllosilicates.

Additional size-fractionation of fine silt was performed to improve insight into mineral weathering features. Figures 7b-d show X-ray diffraction patterns (5-15°2θ) for 10-20, 5-10 and 2-5 µm-fine silt subfractions, respectively. In the 10-20 µm fraction, basal reflections of chlorite ((001), (002)) and of mica (001) occurred distinctly for the basic and reference treatments. In the acid treatments, the intensity of chlorite peaks only little decreased for ammonium sulphate with respect to the reference, but virtually disappeared for di-ammonium phosphate. The *d*(110) peak of amphibole (hornblende), clearly detected for basic and reference plots, strongly diminished for $(NH_4)_2SO_4$, and missed for $(NH_4)_2HPO_4$. Interestingly, although not shown here, acidification by ammonium fertilization affected more particularly Na/Ca-feldspar peaks, in comparison to XRD patterns of the $CaCO_3$ treatment, notably 0.402 and 0.365 nm reflexions typical for plagioclase (Moore and Reynolds,

1997). In the 5-10 and 2-5-µm fractions, the basal reflexions of chlorite were also strongly reduced or absent for $(NH_4)_2HPO_4$. Amphibole peaks were not detected for all treatments (Figure 7c,d). By contrast, for $(NH_4)_2HPO_4$, the intensity of the *d*(001) reflexion of mica was notably stronger in the 2-5-µm-fraction than in the 5-10 and 10-20-µm fractions, suggesting a process of mineral particle breakdown under strong acidified soil conditions. Such findings were consistent with a hypothesis of recharge of the soil clay fraction by primary phyllosilicate minerals (chlorite, mica) due to their microdivision in the fine silt fraction (Hardy et al., 1999). The difference between partial ($(NH_4)_2SO_4$) or total ($(NH_4)_2HPO_4$) mineral dissolution was ascribed to the complexation action by phosphate of Al, liberated by weathering, favouring complete mineral dissolution; for ammonium sulphate, liberated Al may occupy phyllosilicate-interlayers and favour the formation of secondary chlorite-like minerals. Nevertheless, such processes of mineral breakdown and particle transfer from coarser to finer silt fractions, and *in fine,* to the clay fraction, are difficult to unravel by means of X-ray diffraction.

3.3 Indicators for accelerated soil forming processes and pedogenesis

3.3.1 Natural soil chronosequences on loess under temperate climatic conditions

After an initial stage of carbonate dissolution followed by decalcification, the clay migration process primarily characterizes the soil evolution on aeolian loess formations in Europe (Jamagne, 1973, 2011). With time, this process generates growing textural and structural contrast between the eluvial E and illuvial Bt horizons, enhancing temporary water logging. Such hydromorphic, and attending acidified, soil conditions produce clay destruction in the upper part of the Bt horizon, and downward tonguing of the E horizon (Jamagne and Begon, 1984; Jamagne et al., 1984) with a related soil chronosequence Eutric Cambisol → Haplic Luvisol → Retisol. Further intense soil acidification may engender podsolization processes at the soils surface (Brahy et al., 2000), driving a Retisol-'incipient micropodzol' development.

3.3.2 Indicators of amplified clay translocation under prolonged inputs of Na/K fertilizers

In France, contemporary impacts of human activity on clay composition and distribution patterns in Luvisols were recently studied in case of changing land use (Sauzet et al., 2016), drainage conditions (Montagne et al., 2013; Cornu et al., 2007, 2017), or centenary wastewater discharge (Thiry et al., 2013; van Oort et al., 2008, 2017b). However, all these works referred to preliminary comprehensive field surveys in soil pits or trenches, a basic study-step proscribed in the case of the 42-plots experiment with respect to the small size of the plots. In our work, micromorphology study provided first qualitative indication for contemporary clay illuviation in subsurface horizons under Na- and K-based fertilization (Figure 6). Quantitative evidence for an amplification of the clay leaching process can be obtained by calculating textural differentiation indexes (TDI) (Figure 8). Although such texture contrasts in Luvisols are generally established with respect to the eluvial E horizon (Baize, 2018), we here calculated TDI with reference to the Ap horizon, the surface layer being primarily impacted by fertilization and related modified exchangeable cation compositions (Figure 4). At the scale of the solum, the TDI between the Ap and the most clay-rich Bt horizons showed values close to 1.5 for the basic, ammonium and reference plots (Figure 8a), referring in the French 'Référentiel Pédologique' (RPF) typology (AFES, 2009) to 'NÉOLUVISOLS', in the FAO classification system to Eutric Luvisols (IUSS Working Group WRB. 2015). For monovalent Na & K treatments, the TDI increased to 1.7 for KCl, 1.8 for sylvinite and to 2.2 for $NaNO_3$. In the RPF system, a TDI > 1.8 and 10-30% clay in the eluvial horizon refers to 'LUVISOLS TYPIQUES' (AFES, 2009) or Haplic Luvisols (IUSS Working Group WRB. 2015). Moreover, additional field observation outlined periodically water stagnation at the surface of the Na and K plots following each significant rainfall event, leading to clay and soil structure degradation, and a premise for the development of Retisols and some Planosols.

Between the surface Ap and the underlying E horizon, strong increasing textural differentiation was observed for monovalent treatments, to about 1.5 for K-based fertilizers and to 1.8 for $NaNO_3$ (Figure 8b), in comparison to the TDI values of ≈ 1.1-1.2 for basic and acid NH_4- based treatments.

Reference plots showed a TDI close to 1.3. These findings clearly attested for a contemporary and short-range intensification of clay migration out from the surface horizon. Interestingly, when compiling TDI data conventionally, *i.e.* comparing the clay contents of the eluvial E and the most clay-rich Bt horizon, little or no difference was found between the different fertilization treatments (Figure 8c). Our findings on notable increasing TDI's since 4 or 5 decades (Figure 3a) gave clear evidence for an amplified clay transfer, boosted by prolonged inputs of Na/K-based fertilizers. So far these transfers concern primarily clay eluviation from the Ap and its illuviation in the E horizon, but also such clay translocation also already affects deeper E/Bt and Bt horizons, as shown by the presence of contemporary thick clay coatings (Figure 6).

3.3.3 Indicators of soil acidification and corollary mineral weathering

Late-Weichselian loess formations in northern France contain predominantly quartz (60-70%), and notable amounts of Na-Ca plagioclase, K-feldspars, mica (muscovite, biotite), chlorite, and clay minerals (smectite, vermiculite, illite, and kaolinite). In addition, they include trace amounts of heavy minerals (epidote, amphibole, garnet), with proportions depending on the geological source basins of Pleistocene aeolian silt and sand covers in north-western Europe (Jamagne, 1973; Antoine, 2002; Antoine et al., 2003). According to Goldich (1938), ranking the resistance of mineral groups to weathering, ferromagnesian amphiboles (hornblende) and phyllosilicates (biotite, chlorite) weather more rapidly than dioctahedral mica (muscovite), Ca-rich feldspars more rapidly than Na-rich ones and plagioclase more rapidly than potassium feldspars (Figure 9).

Mineral weathering depends on a wide panel of physicochemical, biochemical and hydrodynamic soil parameters (Wilson, 2004). Although weathering rates are arduous to generalize, orders of magnitude have been established for ferromagnesian silicates and feldspars under controlled experimental conditions assumed to mimic real field conditions. Dissolution times of decades to one century have been calculated for chlorite, biotite and for the calcium feldspar anorthite (Kodama et al., 1983; Lasaga, 1984; Wilson, 2004), a time span compatible with the duration of the 42-plots

experiment. Many workers stressed the role of low pH and organic acids in intensifying mineral weathering. Thus, vermiculitization was mentioned as a ''simple form of weathering of biotite and chlorite" (Wilson, 2004), but under more intensive weathering conditions, they may convert directly to kaolinite. However, under strong acidic conditions and favoured by complexing organic acids, ferromagnesian minerals may be completely dissolved (Robert et al., 1980a,b; Drever and Stillings, 1997), a major soil forming process in Podzols (van Breemen and Buurman, 2013). In our work, under di-ammonium phosphate additions, phosphate apparently replaces the role of complexing organic agents in strong acidified soil conditions, favouring a quasi-complete dissolution of ferromagnesian minerals, as was demonstrated by XRD work (Figure 7). These findings evoke conditions close to those of the acidocomplexolysis process (Pédro, 2018), typical for Podzols.

During experimental weathering of ferromagnesian minerals, substantial amounts of constitutive Mg, Fe, and Al were liberated (Kodama et al., 1983). In Late Weichselian loess formations in north-western Europe, the main reserve of weatherable primary minerals is located in the silt fraction (Pésci, 1990, Antoine et al., 2003), notably present in fine silt (Hardy et al., 1999). We therefore analysed the major element compositions in the silt fractions (Figure 10) to support XRD findings on mineralogical alterations issued by prolonged ammonium fertilizers (Figure 7). The concentrations of Mg, Fe and Al were clearly lower in A, E and Bt horizons under NH_4-additions, compared to the reference and $CaCO_3$ plots. Their concentration patterns showed remarkable mutual similarities (Figure 10), but also regarding their respective pH-profiles (Figure 2d). Moreover, both concentration-deviations and total concentrations decreased from the finest to the coarsest fine silt fractions (Figure 10 a-c). Although Mg, Fe, and Al are not exclusively constitutive of ferromagnesian phyllosilicates and amphiboles, their concentration patterns strongly advocate for an increased weathering intensity under acidified soil conditions within an infra-decennial time-span, preferentially affecting the finest fine-silt fractions. Interestingly, the concentration profile of scandium (Sc), showed remarkable similarities with the distribution patterns of Mg, Fe and Al

concentrations (Figure 10). Scandium, a rare earth trace element, was used in previous work to validate geochemical budget calculations for major and trace elements in surface horizons of all 42 plots since the start of the experiment (van Oort et al., 2017a, 2018). In loess soils, scandium was mentioned to occur quasi-exclusively in ferromagnesian amphibole-hornblende, chlorite and biotite (Mitchell, 1964; Das et al., 1971; Horovitz et al., 1975; Hocquard, 2003; Aide et al., 2009), due to its frequent substitution with iron, eased by comparable ion radius (Sc: 0.075 nm, Fe^{2+}: 0.076 nm, Fe^{3+}: 0.064 nm). Therefore, scandium concentrations may represent a highly valuable indicator for weathering of ferromagnesian minerals. Moreover, varying Sc contents in Luvisols was linked to translocation of phyllosilicate clays (Horovitz et al., 1975), and correlated with structural iron (van Oort, 2018). Hence, scandium may also represent a useful indicator for the clay leaching process.

By contrast, the soil-depth distribution profiles of sodium and potassium presented somewhat higher Na and K concentrations in acid ammonium treatments than in reference and $CaCO_3$ plots (Figure 10). This tendency may indicate a relative accumulation of more resistant Na/K-feldspars in acid soil conditions, at the expense of calcium-rich feldspars, in accordance with Goldich's mineral stability series (Figure 9). The effect was more distinct for Na than for K, as beyond potassium feldspars, a notable amount of K occurs in micas, including resistant muscovite and more weatherable biotite. The strong increase of Ca concentrations in the finest silt fractions at the surface horizon under liming amendments denoted the precipitation of calcium carbonate, promoting soil aggregation and increasing soil structure stability (Paradelo et al., 2013, 2016). However, lower Ca concentrations in the ammonium treatments with respect to the reference plot also suggested an increased dissolution of Ca-rich feldspars. In this respect, geochemical budgets established for the 1928-2014 period (van Oort et al., 2018) showed a net loss of Ca from the surface horizons as high as –1.5 kg m^{-2} for the ammonium fertilization treatments and –1.2 kg m^{-2} for the reference plots. These losses represent almost twice the amounts of calcium removed by lixiviation of exchangeable Ca_{exch} from the CEC, thus attesting for a process of mineral dissolution of Ca-rich plagioclase.

4. CONCLUSIONS

The large historical sample collection of INRAE's long-term bare fallow experiment allowed us to depict accurately the temporal changes of soil physicochemical properties constrained by prolonged fertilization in the surface horizon of a loess Luvisol. They were compared with current soil-depth parameter profiles, studied on subsurface samples from E, B and C -horizons. The options taken at the start of the 42-plots trial, a continuously application of NPK inputs on the same plots, and a bare fallow management, exacerbated the effects of fertilization treatments on major soil characteristics, in accordance with the initial objectives reported in 1939 by Burgevin and Hénin. It may be clear that a straightforward comparison between bare-fallow soils and agricultural soils in real field conditions is precarious. However, the experimental design of the 42-plots trial offered valuable insight into hazards of intensive agriculture on soil forming processes and soil development in loess Luvisols under intensive agriculture with strongly lowered organic carbon contents at a centenary timespan. Such findings are relevant for agricultural areas under intensive crop production, where anthropogenic impacts on the solid soil phases are yet partially buffered and masked by the low reactive OM stocks.

During the first decades of the experiment, decreasing OM contents and rationally the associated biological activity, rapidly engendered soil acidification, loss of exchangeable charges and divalent alkaline earth cations. A diminishing OM-buffering capacity facilitated an increasing control of diverging physicochemical conditions on soil characteristics and properties: fertilization led to growing contrasting exchangeable cation compositions, promoting the acceleration of soil-forming processes.

Thus, Na/K-based fertilizers enhanced clay eluviation from the surface to deeper E and E/Bt horizons, amplifying the Luvisol texture contrast, causing temporal anaerobic conditions and water logging, evolving to a Stagnic Luvisol and on the long-term, to a Retisol. The NH_4-based fertilizers

promoted strong soil acidification (current pH ≈3.5), a total loss of exchangeable calcium and quasi-complete saturation of the soil's exchange complex by Al. X-ray-diffraction attested for weathering in fine silt fractions of ferromagnesian minerals (chlorite, hornblende) and geochemical analyses for weathering of Ca-rich plagioclase. Particularly under inputs of di-ammonium phosphate, acidification caused a quasi-total dissolution of ferromagnesian minerals, the phosphate anion likely playing the role of free Al-complexing organic acids in the acidocomplexolysis process in Podzols. In this view, 85 years of fertilization with $(NH_4)_2HPO_4$ promoted the development of a podsolization-like process in the surface horizon. Moreover, acidification also affected subsurface horizons, sometimes as deep as the carbonated loess parent material. By contrast, basic liming treatments counteracted processes of acidification and clay translocation, and apparently stopped soil development.

In plots without fertilizer inputs, initially defined as 'reference plots', a steady process of alteration developed under temperate climatic conditions of northern France. The current state of these reference plots neither reflect the initial soil conditions at the start of the experiment, nor those of soils under intensive agricultural use. Nevertheless, they were very useful for the study of organic matter decay rates and speeds, the modelling the persistent organic carbon pool, or estimating total amounts of atmospheric trace metal deposition in the Paris suburban region since the 1930s. Effects of climatic acidification affected mainly the surface horizon of the reference plot soil, with ≈ 20-25 % of the exchange complex occupied by Al. However, although suspected by geochemical analyses, clear evidence for weathering of primary ferromagnesian minerals and Ca-rich feldspar was not supported by XRD analyses.

Conclusively, one might consider INRAE's 42-plots LTBF experiment to perform as an 'alert launcher' tool, forecasting risks of soil degradation in OM-depleted soils under intensive agriculture land use. With reverse reasoning, the results of this experiment strongly advocate for preserving and restore organic matter stocks in soils, in terms of quantity, quality and dynamics so to limit risks of

soil degradation and to guarantee the sustainability of invaluable ecosystem services delivered by soils to humankind.

5. Acknowledgements

The authors gratefully acknowledge a long list of INRA personnel, involved in one way or another in the 42-plots experiment, guaranteeing annual field maintenance, inputs of fertilizers and amendments, di-annual digging, removal of weeds, soil sampling, and preparation and archiving of soil samples. Currently, this work is to a large part carried out by Sébastien Breuil over the last ten years. The present synthetic work on the impacts of long-term fertilization on soil nature and properties would not have been possible without all their continuous efforts during 9 decades. Many thanks to you all! Many thanks to Christian Le Lay (INRAE-Orléans) for preparing a large series of soil thin sections. We acknowledge financial support from INRAE's 'AgroEoSystem' department and from the French 'Agence de l'Environnement et de la Maîtrise de l'Energie', (ADEME, 14-60-C0064). Remigio Paradelo acknowledges a 'Ramón y Cajal' fellowship (RYC-2016-19286) from the Spanish Ministry of Economy and Competitiveness (MINECO).

References

AFES, 2009. Référentiel pédologique 2008. Editions Quae, Versailles, France, 405p.

Aide, M., Braden, I., Mueler, W. 2009. Partitioning of iron and scandium in soils having water drainage limitations. Appl. Environ. Soil Sci., Article ID 243482.

Andreoli, C.Y. 1989. Evolution des phyllosilicates 2/1 en fonction de la dynamique du potassium. Thesis, Pierre et Marie Curie University, Paris-VI, 233 pp.

Andreoli, C.Y., Robert, M., Pons, C.H. 1989. First steps of smectite-illite transformation with humectation and desiccation cycles. Appl. Clay Sci., 4, 1–13.

Antoine, P.L. 2002. Les lœss en France et dans le Nord-Ouest de l'Europe. Rev. Fr. Géotech., 99, 3–21.

Antoine, P.L., Catt, J., Lautridou, J.P., Sommé, J. 2003. The loess and coversands of northern France and southern England. J. Quat. Sci., 18, 309–318.

Arrouays, D., Balesdent, J., Germon, J.C., Jayet, P.A., Soussana, J.F., Stengel, P. 2002. Contribution à la lutte contre l'effet de serre, Stocker du carbone dans les sols agricoles de France ?, Rapport d'expertise scientifique de l'INRA à la demande du Ministère de l'Ecologie et du Développement Durable, Editeurs scientifiques, 334p.

Baize, D. 2018. Guide des analyses en pédologie, 3ième Ed. Quae Editions, Versailles, 328p.

Barnhisel, R.I., Bertsch, P.M. 1989. Chlorites and hydroxy-interlayered vermiculite and smectite. *In*: J.B. Dixon & S.B. Weed (eds.), Minerals in soil environments (2nd Edition). Soil Sci. Soc. Am., Madison (WI), pp. 722–788

Barré, P., Eglin, T., Christensen, B.T., Ciais, P., Houot, S., Kätterer, T., van Oort, F., Peylin, P., Poulton, P.R., Romanenkov, V., Chenu, C. 2010. Quantifying and isolating stable carbon using long-term bare fallow experiments. Biogeosciences, 7, 3839–3850.

Barré, P., Plante, A.F., Cécillon, L., Lutfalla, S., Baudin, F., Bernard, S., Christensen, B.T., Fernandez, J.M., Houot, S., Kätterer, T., Le Guillou, C., Macdonald, A., van Oort, F., Chenu, C. 2016. The energetic and chemical signatures of persistent soil organic matter. Biogeochemistry, 130, 1–12.

Barré, P., Quénéa, K., Vidal, A., Cécillon, L., Christensen, B. T., Kätterer, T., Macdonald, A., Petit, L., Plante, A.F., van Oort, F., Chenu, C. 2018. Microbial and plant-derived compounds both contribute to persistent soil organic carbon in temperate soils. Biogeochemistry, 14 (1), 81–92.

Bolt, G.H., Bruggenwert, M.G.M. 1976. Soil Chemistry. A. Basic Elements. Developments in Soil Science 5A, 2nd Ed. Elsevier, Amsterdam, 281 p.

Bouman, O.T., Curtin, D., Campbell, C.A. Biederbeck, V.O., Ukrainetz, H. 1995. Soil acidification from long-term use of anhydrous ammonia and urea. Soil Sci. Soc. Am., 59, 1488–1494.

Brahy, V., Titeux, H., Delvaux, B. 2000. Incipient podzolization and weathering caused by complexation in a forest Cambisol on loess as revealed by a soil solution study. Eur. J. Soil Sci., 51, 475-484.

van Breemen, N., Buurman, P. 2013. Soil Formation. Springer, Dordrecht, The Netherlands, 377p.

van Breemen, N., Mulder, J., Driscoll, C.T. 1983. Acidification and alkalinization of soils. Plant and Soil, 75, 283–308.

Bresson, L.M., Boiffin, J. 1990. Morphological characterization of soil crust development stages on an experimental field. Geoderma, 47, 301–325.

Burgevin, H., Hénin, S. 1939. Dix années d'expériences sur l'action des engrais sur la composition et les propriétés d'un sol de limon. An. Agron., 9, 771–799.

Cécillon, L., Baudin, F., Chenu, C., Christensen, B.T., Houot ,S., Kätterer, T., Lutfalla, S., Macdonald, A., van Oort, F., Plante, A.F., Savignac, F., Soucémarianadin, L., Barré ,P. 2018. A model based on Rock-Eval thermal analysis to quantify the size of the centennially persistent organic carbon pool in temperate soils. Biogeosciences, 15, 2835–2849.

Ciesielski, H., Sterckeman, T. 1997a. Determination of CEC and exchangeable cations in soils by means of cobalt hexamine trichloride. Effects of experimental conditions. Agronomie, 17, 1–8.

Ciesielski, H., Sterckeman, T. 1997b. A comparison between three methods for the determination of cation exchange capacity and exchangeable cations in soils. Agronomie, 17, 9–16.

Cornu, S., Montagne, D., Hubert, F., Barré, P., Caner, L. 2017. Evidence of short-term clay evolution in soils under human impacts. Geoscience, 344, 747–757.

Cornu, S., Montagne, D., Maguin, F., LeLay, C., Chevallier, P., Cousin, I. 2007. Influence of human impacts on Albeluvisol analyzed by X-ray microfluorescence: Relative evolution of the transforming front at the tongue scale. Sci. Tot. Environ., 377, 244–254.

Das, H.A., Zonderhuis, J., van der Marel, H.W. 1971. Scandium in rocks, minerals and sediments and its relations to iron and aluminum. *Contr. Min. Petrol.*, **32** (3), 231-244.

Drever, J.I., Stillings, L.L. 1997. The role of organic acids in mineral weathering. Coll. Surf. A: Physicochem. Eng. Aspects, 120, 167–181.

Edzwald, J.K., Toensing, D.C., Chi-Yew Leung, M. 1976. Phosphate adsorption reactions with clay minerals. Environ. Sci. Techn., 10, 485–490.

Eeckman, J.P., Laudelout, H. 1961. Chemical Stability of hydrogen-montmorillonite suspensions. Kolloid-Z., 178, 99–107.

Filipek, T., 2011. Liming, effects on soil properties. In: Gliński, J., Horabik, J., Lipiec, J. (eds) Encyclopedia of Agrophysics. Encyclopedia of Earth Sciences Series. Springer, Dordrecht. https://doi.org/10.1007/978-90-481-3585-1_84

FitzPatrick, E.A. 1993. Soil Microscopy and Micromorphology; Wiley: Chichester, UK, 304p.

Fox, J., Bouchet-Valat, M., 2019. Rcmdr: R Commander. R package version 2.6-1, http://socserv.socsci.mcmaster.ca/jfox/Misc/Rcmdr/.

Gis Sol, 2011. L'état des sols de France. Groupement d'intérêt scientifique sur les sols, 188p. http://www.gissol.fr/RESF/index.php.

Goldich, S.S. 1938. A study of rock weathering. J. Geol., 40, 17–-58.

Haney, R.J. Are fertilizers punishing our soils? 2017. http://e360.yale.edu/features/why-its-time-to-stop-punishing-our-soils-with-fertilizers-and-chemicals/.

Hardy, M., Jamagne, M., Elsass, F., Robert, M., Chesneau, D. 1999. Mineralogical development of the silt fractions in a podzoluvisol on loess in the Paris Basin (France). Eur. J. Soil Sci., 50, 443–456.

Heckman, K., Grandy, A.S., Gao, X., Keiluweit, M., Wickings, K., Carpenter, K., Chorover, J., Rasmussen, C. 2013. Sorptive fractionation of organic matter and formation of organo-hydroxy-aluminium complexes during litter biodegradation in the presence of gibbsite. Geochim. Cosmochim. Acta, 121, 337–683.

Hocquard, C. 2003. Le scandium. Economie et gîtologie BRGM Orléans, 65p.

Horovitz, C.T., Gschneidner, Jr. K.A., Melson, G.A., Youngblood, D.H., Schock, H.H. 1975. Scandium. Its Occurrence, Chemistry, Physics, Metallurgy, Biology and Technology. Acad. Press, London.

Huang, P.M. 2005. Chemistry of potassium in soils. In: Tabatabai, M.A., Sparks, D.L. (Eds.), Chemical Processes in Soils. Soil Sci. Soc. Am., Madison, WI, USA, pp. 227–292.

Isambert, M. 1979. Etudes des Sols des Parcelles Expérimentales du CNRA Versailles, Parcelles des Closeaux. Rapport Interne, SESCPF, INRA-Orléans, France.

IUSS Working Group WRB. 2015. World Reference Base for Soil Resources 2014, update 2015. International soil classification system for naming soils and creating legends for soil maps. World Soil Resources Reports No. 106. FAO, Rome, Italy.

Jackson, M.L., Sherman, G.D. 1953. Chemical weathering of minerals in soils. Adv. Agron., 5, 219-318.

Jamagne, M. 1973. Contribution à l'étude pédogénétique des formations lœssiques du Nord de la France. Thèse d'Etat, Faculté des Sciences Agronomiques de l'Etat, Gembloux (Belgique), 445 p.

Jamagne, M. 2011. Grands paysages pédologiques de France. Éditions Quæ, Versailles, 535p.

Jamagne M., Bégon, J.C. 1984. Les sols lessivés de la zone tempérée. Apports de la pédologie française. A.F.E.S. Livre Jubilaire, 55–76.

Jamagne, M., De Coninck, F., Robert, M., Maucorps, J. 1984. Mineralogy of clay fractions of some soils on loess in northern France. Geoderma, 33, 319–342.

Julien, J.L., Turpin, A. 1999. Surface réactives et raisonnement de quelques propriétés chimiques des sols acides. C. R. Acad. Agr. France, 85, 25–35.

Kabata Pendias, A. 2011. *Trace elements in soils and plants*. 4th Edition, CRC Books, 548pp.

Kodama, H., Schnitzer, M., Jaakkimainen, M. 1983. Chlorite and biotite weathering by fulvic acid solutions in closed and open systems. Can. J. Soil Sci., 63, 619–629.

Kleber, M., Eusterhues, K., Keiluweit, M., Mikutta, C., Mikutta, R., Nico, P.S. 2015. Mineral–organic associations: formation, properties, and relevance in soil environments. Adv. Agron., 13, 1-140

Kögel-Knabner, I., Amelung, W. 2021. Soil organic matter in major pedogenic soil groups. Geoderma, 384, P114785.

Kögel-Knabner, I., Kleber, M. 2011. Mineralogical, Physicochemical, and Microbiological Controls on Soil Organic Matter Stabilization and Turnover. In: Handbook of Soil Sciences: Resource Management and Environmental Impacts, Second Edition, CRC Press, 830 pp.

Kunhikrishnan, A., Thangarajan, R., Bolan, N.S., Gleeson, D.B., Seshadri, B., Zaman, M., Barton, L., Tang, C., Luo, J., Dalal, R., Ding, W., Kirkham, M.B., Naidu, R. 2016. Functional relationships of soil acidification, liming and greenhouse gas flux. Adv. Agr., 139, 1–71.

Lal, R. 2015. Restoring Soil Quality to Mitigate Soil Degradation. Sustainability, 7, 5875–5895.

Lasaga, A.C. 1984. Chemical kinetics of water-rock interactions. J. Geoph. Res., 89, 4009-4025.

Le Bissonnais, Y., Benkhadra, H., Chaplot, V., Gallien, E., Eimberck, M., Fox, D., Martin, P., Ligneau, L., Ouvry, J.F. 1996. Genèse du ruissellement et de l'érosion diffuse des sols limoneux : analyse du transfert d'échelle du m² au versant. Géomorphologie : relief, processus, environnement, 2–3, 51–64.

Lefèvre, R., Barré, P., Moyano, F.E., Christensen, B.T., Bardoux, G., Eglin, T., Girardin, C., Houot, S., Kätterer, T., van Oort, F., Chenu, C. 2014. Higher temperature sensitivity for stable than for labile soil organic carbon - Evidence from incubations of long-term bare fallow soils. Glob. Change Biol., 20, 633–640.

Levy, G.J., Torrento, J.R. 1995. Clay dispersion and macroaggregate stability as affected by exchangeable potassium and sodium. Soil Sci., 160, 352–358.

Lutfalla, S., Abiven, S., Barré, P., Wiedemeier, D.B., Christensen, B.T., Houot, S., Kätterer, T., Macdonald, A., van Oort, F., Chenu, C. 2017. Pyrogenic carbon lacks long-term persistence in temperate arable soils. Front. Earth Sci., 5, 1–10.

Menichetti, L., Houot, S., van Oort, F., Kätterer, T., Christensen, B.T., Chenu, C., Barré, P., Vasilyeva, N., Ekblad, A. 2015. Increase in soil stable carbon isotope ratio relates to loss of organic carbon: results from five long-term bare fallow experiments. Oecologia, 177, 811–821.

Mitchel, R.L. 1964. Trace elements in soils. In: F.E. Bear (ed) Chemistry of the soil. 2nd Ed. Rheinholt, New York.

Moni, C. 2008. Stabilisation Physique et Physico-Chimique de la Matière Organique dans les Horizons Profonds du Sol. Ph.D. Thesis, Université Pierre et Marie Curie, Paris, France.

Montagne, D., Cousin, I., Josière, O., Cornu, S. 2013. Agricultural drainage-induced Albeluvisol evolution: A source of deterministic chaos. Geoderma, 193–194, 109–116.

Montanarella, L. 2010. Moving Ahead from Assessments to Actions: Could We Win the Struggle with Soil Degradation in Europe? *In*: Zdruli P., Pagliai M., Kapur S., Faz Cano A. (eds), Land Degradation and Desertification: Assessment, Mitigation and Remediation, pp. 15–23. Springer, Dordrecht.

Moore, D.M., Reynolds Jr, R.C. 1997. X-ray diffraction and the identification of clay minerals. 2nd Edition. Oxford University Press, New York, 378 p.

Oades, J.M. 1984. Soil organic matter and structural stability: mechanisms and implications for management. Plant and Soil, 76, 319–337.

Oberti, R., Boiocchi, M., Hawthorne, F.C., Marco, C.E. 2018. Magnesi-hornblende from Lüderitz, Namibia: mineral description and crystal chemistry. Min. Mag., 82, 1253–1259.

van Oort, F. 2018. Cinétique Centenaire d'Évolution de Propriétés de Sols de Lœss appauvris en matières organiques. Etat des lieux de 85 ans d'expérimentation d'impacts de fertilisation sur les sols de limon dans le dispositif des 42 parcelles à l'Inra de Versailles (1929–2014). 150p. www.ademe.fr/mediatheque

van Oort, F., Jongmans, A.G., Lamy, I., Baize, D., Chevallier, P. 2008. Impacts of long-term wastewater irrigation on the development of sandy Luvisols: consequences for metal pollutant distributions. Eur. J. Soil Sci., 59, 925–938.

van Oort, F., Labanowski, J., Jongmans, T., Thiry, M. 2007. Le devenir des polluants métalliques dans les sols : révélateur d'impacts de l'activité humaine sur la pédogenèse? Etud. Gest. Sols, 14, 287–303.

van Oort, F., Paradelo, R., Monna, F., Chenu, C., Guérin, A., Breuil, S., Delarue, G., Thoisy, J.C., Proix, N. 2020b. La collection historique d'échantillons de l'essai patrimonial dit des 42 parcelles d'INRAE à Versailles : une machine à remonter le temps... Etud. Gest. Sols, 27, 321–350.

van Oort, F., Paradelo, R., Proix, N., Baize, D., Breuil, S., Foy, E., Guérin, A., Monna, F. 2020a. En direct de l'essai patrimonial des 42 parcelles de l'INRA de Versailles : les impacts de fertilisations centenaires en profondeur du Néoluvisol de lœss. Etud. Gest. Sols, 27, 163–187.

van Oort, F., Paradelo, R., Proix, N., Breuil, S., Delarue, G., Trouvé, A., Baize, D., Monna, F., Richard, A. 2017a. Arsenic et Vieilles Parcelles. Etats et bilans géochimiques dans l'horizon de surface d'un Néoluvisol de lœss nu, avec ou sans apports de matières fertilisantes depuis 1928. Étud. Gest. Sols, 24, 99–126.

van Oort, F., Paradelo, R., Proix, N., Delarue, G., Baize, D., Monna, F. 2018. Centennial fertilization-induced soil processes control trace metal dynamics. Lessons from a long-term bare fallow experiment. Soil Syst., 2, 23.

van Oort, F., Proix, N., Paradelo, R., Delarue, G., Breuil, S., Baize, D., Richard, A. 2016. Dernières nouvelles de 42 vieilles parcelles. Indicateurs d'évolutions pédologiques infra-centenaires en Néoluvisol de lœss nu, sous contrainte d'applications continues de matières fertilisantes. Étud. Gest. Sols, 23, 143–162.

van Oort, F., Thiry, M., Foy, E., Fujisaki, K., Delarue, G., Dairon, R., Jongmans, T. 2017b. Impacts of one century of wastewater discharge on soil transformation through ferrolysis and related metal pollutant distributions. Sci. Tot. Environ., 590-591, 1–13.

Paradelo, R., van Oort, F., Chenu, C. 2013. Water-dispersible clay in bare fallow soils after 80 years of continuous fertilizers addition. Geoderma, 200–201, 40–44.

Paradelo, R., van Oort, F., Barré, P., Billiou, D., Chenu, C. 2016. Soil organic matter stabilization at the pluri-decadal scale: Insight from bare fallow soils with contrasting physicochemical properties and macrostructures. Geoderma, 275**,** 48–54.

Paradelo, R., Virto, I., Chenu, C. 2015. Net effect of liming on soil organic carbon stocks: a review. Agric. Ecosyst. Environ., 202**,** 98-107.

Parfitt, R.L., 1978. Anion adsorption by soils and soil solution. Adv. Agr., 30, 1–50.

Pédro G. 2018. Les couvertures superficielles des espaces continentaux de la terre ? Regards sur les inégalités territoriales naturelles de la planète. AFES, Orléans, 170 p.

Pernes-Debuyser, A., Pernes, M., Velde, B., Tessier, D. 2003. Soil mineralogy evolution in the INRA 42 plots experiment (Versailles, France). Clays Clay Min., 51, 577–584.

Pernes-Debuyser, A., Tessier, D. 2002. Influence de matières fertilisantes sur les propriétés des sols : cas des 42 parcelles de l'INRA à Versailles. Étud. Gest. Sols, 9, 177–186.

Pésci, M. 1990. Loess is not just the accumulation of dust. Quat. Int., 7/8, 1–21.

R Core Team, 2019. R: A language and environment for statistical computing. Vienna, Austria: R Foundation for Statistical Computing. https://www.R-project.org/

Robert, M., Razzaghe, M., Vicente, M. A., Veneau, G. 1980a. Rôle du facteur biochimique dans l'altération des minéraux silicatés. Sci. Sol, 2, 161–175.

Robert, M., Veneau, G., Berrier, J. 1980b. Solubilisation comparée des silicates, carbonates et hydroxydes en fonction des conditions du milieu. Bull. Min., 103, 324–329.

Rowley, M.C., Grand, S., Verrecchia, E.P. 2018. Calcium-mediated stabilization of soil organic carbon. Biogeochem., 137, 27–49.

Sauzet, O., Cammas, C., Barbillon, P., Étienne, M.P., Montagne, D. 2016. Illuviation intensity and land use change: Quantification via micromorphological analysis. Geoderma, 266, 46–57.

Scheel, T., Jansen, B., van Wijk, A. J., Verstraten, J.M., Kalbitz, K. 2008. Stabilization of dissolved organic matter by aluminium: a toxic effect or stabilization through precipitation? Eur. J. Soil Sci., 59, 1122–1132.

Six, J., Bossuyt, H., Degryze, S.D., Denef, K. 2004. A history of research on the links between (micro)aggregates, soil biota and soil organic matter dynamics. Soil Till. Res., 79, 7–31.

Sparks, D.L. 2003. Environ. Soil Chem. Acad. Press, Cambridge, USA, 352 p.

Sposito, G. 1989. The Environmental Chemistry of Aluminum. CRC Press, Boca Raton, Fl., 317 p.

Stoops, G. 2003. Guidelines for analysis and description of soil and regolith thin sections. Madison WI, SSSA Inc.

Stoops, G., Marcellino, V., Mees, F. 2010. Interpretation of micromorphological features of soils and regolith. Elsevier, Amsterdam.

Takahashi, T., Dahlgren, R.A. 2016. Nature, properties and function of aluminum-humus complexes in volcanic soils. Geoderma, 263, 110–121.

Talibudeen, O. 1981. Cation exchange in soils. *In*: D.J. Greenland, M.H.B. Hayes (eds.), The chemistry of soil processes. John Whiley & Sons, Chichester, pp. 115–177.

Tessier, D. 1990. Behaviour and microstructure of clay minerals. Soil Colloids and Their Associations in Aggregates; In: M.F. De Boodt, M.H.B. Hayes & A. Herbillon (eds). NATO ASI Series B: Physics; Plenum Press: New York, NY, USA, pp. 387–415.

Thiry, M., van Oort, F., Thiesson, J., van Vliet-Lanoë, B. 2013. Periglacial morphogenesis in the Paris Basin: insight from geophysical prospection and impacts on the fate soil pollution. Geomorphology, 197, 34–44.

Wilding, L.P., Tessier, D. 1988. Genesis of Vertisols: shrink-swell phenomena. In: L.P. Wilding, R. Puentes (eds), Vertisols: their distribution, properties, classification and management. Technical Monograph, n° 18, Texas A&M University Printing Center, TX, pp. 55–81.

Wilson, M.J. 2004. Weathering of the primary rock-forming minerals: processes, products and rates. Clay Min., 39, 233–266.

Wuddivira, M., Camps-Roach, G. 2006. Effects of organic matter and calcium on soil structural stability. Eur. J. Soil Sci., 58, 722–727.

FIGURE CAPTION

Fig. 1. Left, an overview of the 42-plots experiment; middle, a sample collected on July 22, 1929 from plot n°15; right, view of archived samples (photos Sébastien Breuil).

Fig. 2. Temporal evolution in surface horizons of organic carbon (OC) contents (a) and pH (c) from 1929 to 2014 and related soil-depth concentration profiles in 2015 (b,d). Fertilization treatments: ammonium sulphate (P2), di-ammonium phosphate (P14), calcium carbonate (P39), basic slag (P35), sodium nitrate (P4), sylvinite (P29), potassium chloride (P23), ref: means of reference plots P9 and P34 with maximum/minimum value bars.

Fig. 3. Temporal evolution in surface horizons of cation exchange capacities (CECCohex) (a) and clay contents (c) from 1929 to 2014 and related soil-depth concentration profiles in 2015 (b,d). Fertilization treatments: ammonium sulphate (P2), di-ammonium phosphate (P14), calcium carbonate (P39), basic slag (P35), sodium nitrate (P4), sylvinite (P29), potassium chloride (P23), ref: means of reference plots P9 and P34 with maximum/minimum value bars.

Fig. 4. Temporal evolution in surface horizons of exchangeable cations. Fertilization treatments: ammonium sulphate (P2), di-ammonium phosphate (P14), ref: means of reference plots P9 and P34, calcium carbonate (P39), basic slag (P35), potassium chloride (P23), sylvinite (P29), sodium nitrate (P4).

Fig. 5. Soil-depth evolution of exchangeable cation compositions. Fertilization treatments: a) ammonium sulphate (P2), b) di-ammonium phosphate (P14), c) ref: means of reference plots P9 and P34,d) calcium carbonate (P39), e) basic slag (P35), f) potassium chloride (P23), g) sylvinite (P29), h) sodium nitrate (P4).

Fig. 6. Optical microscopy photographs of contemporary pedofeatures in subsurface soil horizons under selected fertilization treatments. (a) laminated and layered clay coatings, $NaNO_3$ plot, 40-50 cm, (b) idem, 70-80-cm depth; (c) compound layered dusty clay-silt coatings, $NaNO_3$ plot, 30-40-cm depth, (d) idem, sylvinite plot, 30-40-cm depth; (e) dusty, poorly sorted clay-silt coatings (matrans, arrows), reference plot, 30-40-cm depth, (f) idem, ammonium sulphate plot 30-40-cm depth; (g) manganese impregnation of pore-walls (hypocoatings), ammonium sulphate plot, 60-70-cm depth, (h) idem, 70-80-cm depth; (i) dendritic manganese nodules (black arrow), di-ammonium phosphate plot, 45-55-cm depth. V: voids. Photos in crossed polarized light (a, b, d), half crossed polarized light (e-h), or plain polarized light (c, i).

Fig. 7. X-ray diffraction diagrams of oriented fine silt fractions form 2014 surface horizon samples, after 85-year inputs of di-ammonium phosphate (P14) and ammonium sulphate (P2), no-inputs (reference plot P9), or liming amendments with calcium carbonate (P39). (a) global 2-20-µm fraction and fine-silt subfractions 2-5 µm (b), 5-10 µm (c), and 10-20 µm (d). V: Vermiculite, Ch: chlorite, M: mica, Am: amphibole, K: kaolinite.

Fig. 8. Textural Differentiation Index (TDI) calculated for the eight fertilization treatments. a) at the scale of the solum (horizons with the highest/lowest clay contents); b) surface soil contrast between the surface Ap and underlying E horizon; c) conventional TDI between illuvial/eluvial horizons.

Fig. 9. Mineral stability series after Goldich (1938), Jackson and Sherman (1953), setting the resistance to weathering of ferromagnesian amphibole (hornblende) and phyllosilicates (biotite and chlorite) present in loess formations of north-western Europe.

Fig. 10. Soil-depth total concentration profiles of major elements Mg, Fe, Al, Ca, Na, and K and of the trace element Scandium (Sc) determined on sub-fine-silt fractions: 2-5 µm (a), 5-10 µm (b), and 10-20 µm (c) for four fertilization treatments ammonium sulphate (P2), di-ammonium phosphate (P14), non-amended reference (P9), and calcium carbonate (P39).

fertilization	composition	number of plots	equivalent input ($ha^{-1}.y^{-1}$)
nitrogen	ammonium	8	150 kg N
	nitrate (Na, Ca)	4	
	dried blood	2	
potassium	K-based	4	250 kg K_2O
	K/Na-based (sylvinite)	2	
phosphorus	phosphate	4	200 kg P_2O_5
	basic slag	2	
basic amendments	quick lime	2	1000 kg CaO
	calcium-carbonate	2	
organic matter	horse manure	2	100 t
reference	no-input	10	-

Table 1. Details of fertilization design in the 42-plots experiment and equivalent annual input-rates per hectare

plot-n°	designation	fertilization	composition	exch. cations	action	graphic marks
9, 34	reference	no-input	-	-	evolution under local climatic conditions	♦
2	acid	ammonium sulphate	$(NH_4)_2SO_4$	Al^{3+} (← H^+)	acidification, mineral weathering	●
14		di-ammonium phosphate	$(NH_4)_2HPO_4$			■
23	monovalent	potassium chloride	KCl	K^+	clay dispersion and leaching, aggregate breakdown, densification	▩
29		sylvinite	(K,Na)Cl	K^+, Na^+		△
4		sodium nitrate	$NaNO_3$	Na^+		◍
35	basic	basic slag	PO_4, CaO	Ca^{2+}	liming, increase of pH and aggregate stability	□
39		calcium carbonate	$CaCO_3$			○

Table 2. Identification, composition and main effects of selected treatments, legend marks in graphs.

*Table 3. Results of ANOVA for the effect of treatment on soil properties. Significance of the effect of factors is indicated as follows: * significant at a P-value of 0.05; ** significant at a P-value of 0.01; *** significant at a P-value of 0.001. Different letters within each column indicate statistically significant differences between treatments in the Tukey test at p<0.05.*

		pH	*CEC*	*OC (1972-2014)*	*Clay*
Treatment	*F*	*129.9*	*16.2*	*6.9*	*5.0*
	P	*<0.001***	*<0.001***	*<0.001***	*<0.001***
no-input		*b*	*bc*	*ab*	*c*
ammonium sulphate		*a*	*ab*	*bc*	*bc*
di-ammonium phosphate		*a*	*a*	*c*	*cd*
potassium chloride		*bc*	*a*	*a*	*ac*
sylvinite		*bc*	*a*	*a*	*ab*
sodium nitrate		*c*	*ab*	*ab*	*a*
basic slag		*d*	*d*	*bc*	*ac*
calcium carbonate		*d*	*cd*	*bc*	*ac*


a)
b)
c)
STATION CENTRALE
D'AGRONOMIE
Prélèvement N° 15
du 22 Juillet 1929

Fig. 1.

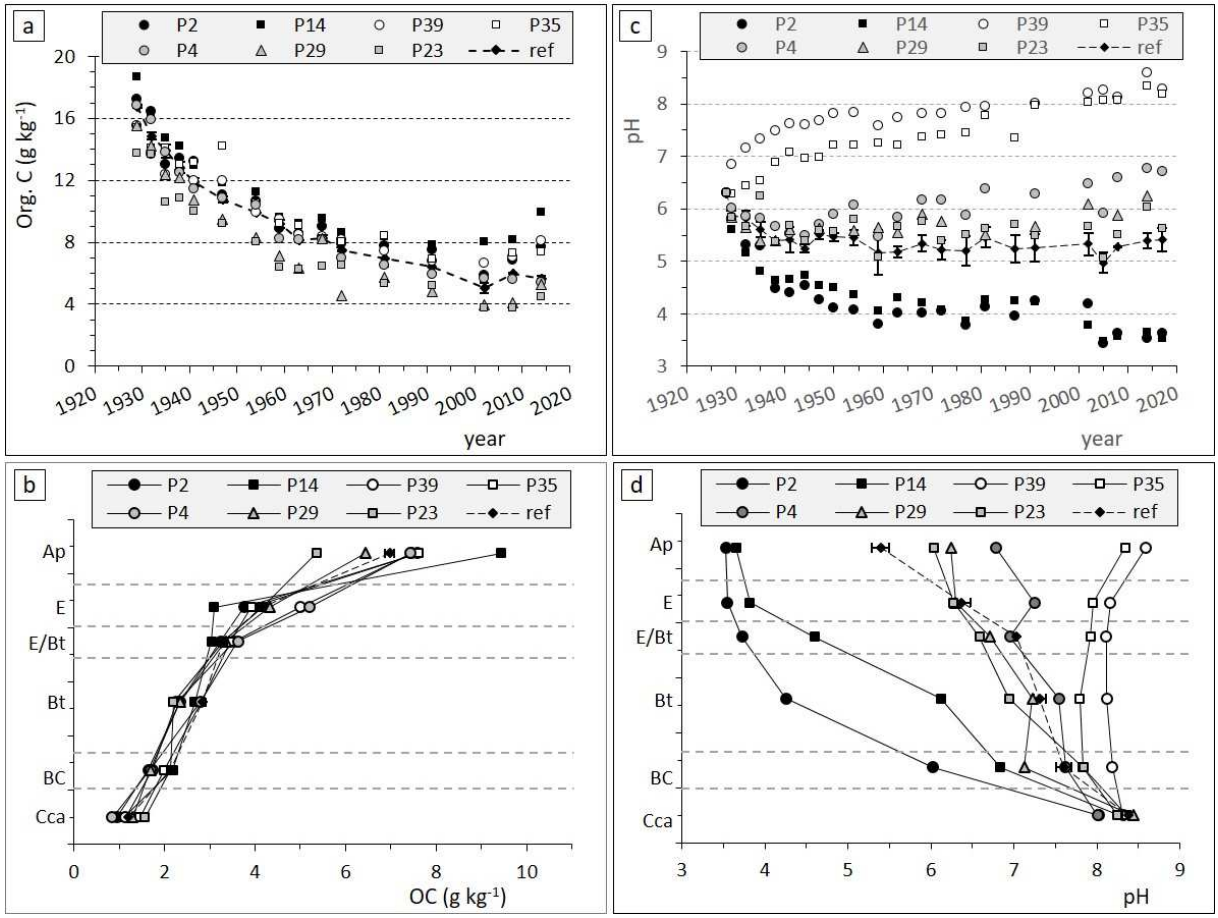
a
P2
P14
P39
P35
P4
P29
P23
ref
Org. C (g kg-1)
year
c
pH
year
b
Ap
E
E/Bt
Bt
BC
Cca
OC (g kg-1)
d
pH

Fig. 2.

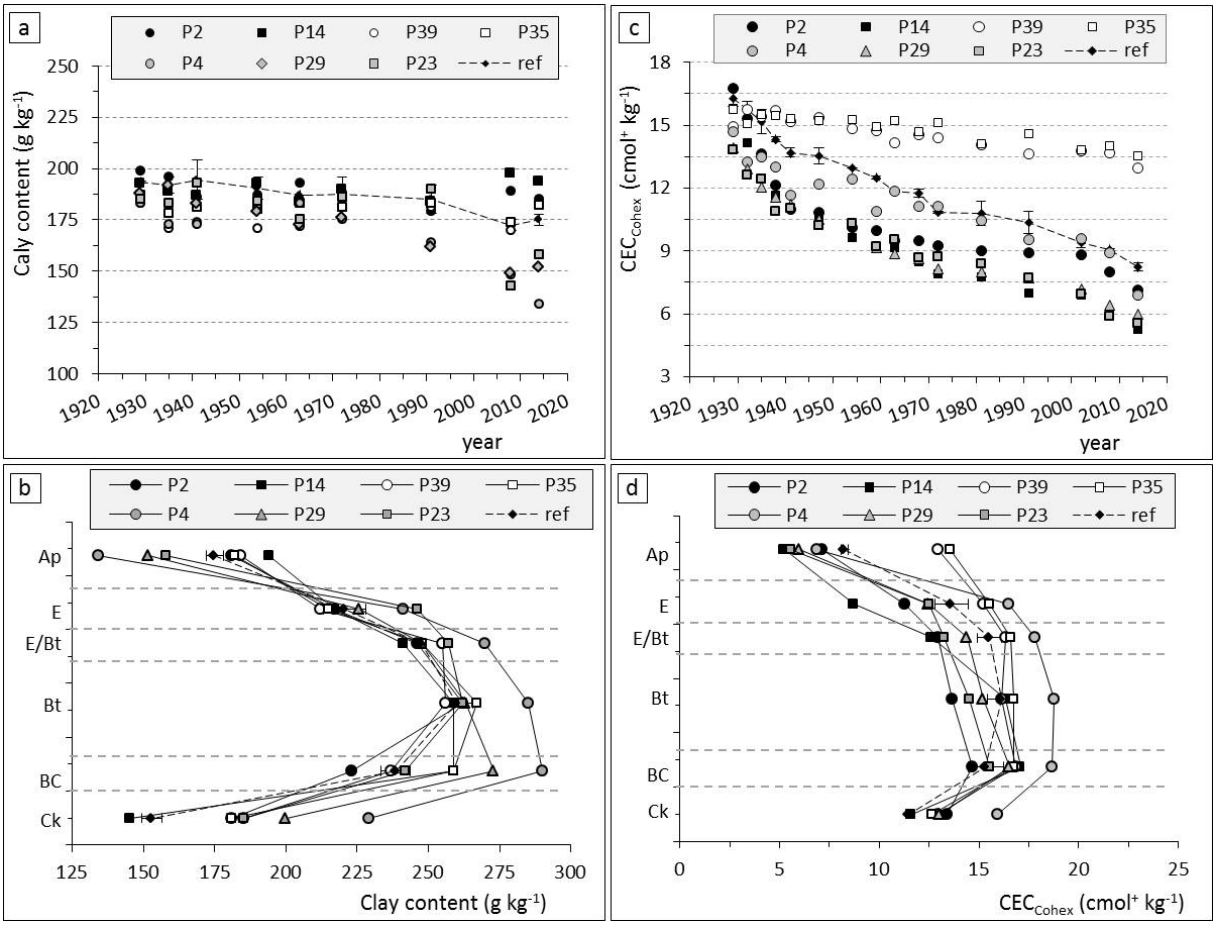
a
P2
P14
P39
P35
P4
P29
P23
ref
Caly content (g kg-1)
250
225
200
175
150
125
100
1920
1930
1940
1950
1960
1970
1980
1990
2000
2010
2020
year
c
CECCohex (cmol+ kg-1)
18
15
12
9
6
3
b
Ap
E
E/Bt
Bt
BC
Ck
125
150
175
200
225
250
275
300
Clay content (g kg-1)
d
0
5
10
15
20
25
CECCohex (cmol+ kg-1)

Fig. 3.

1

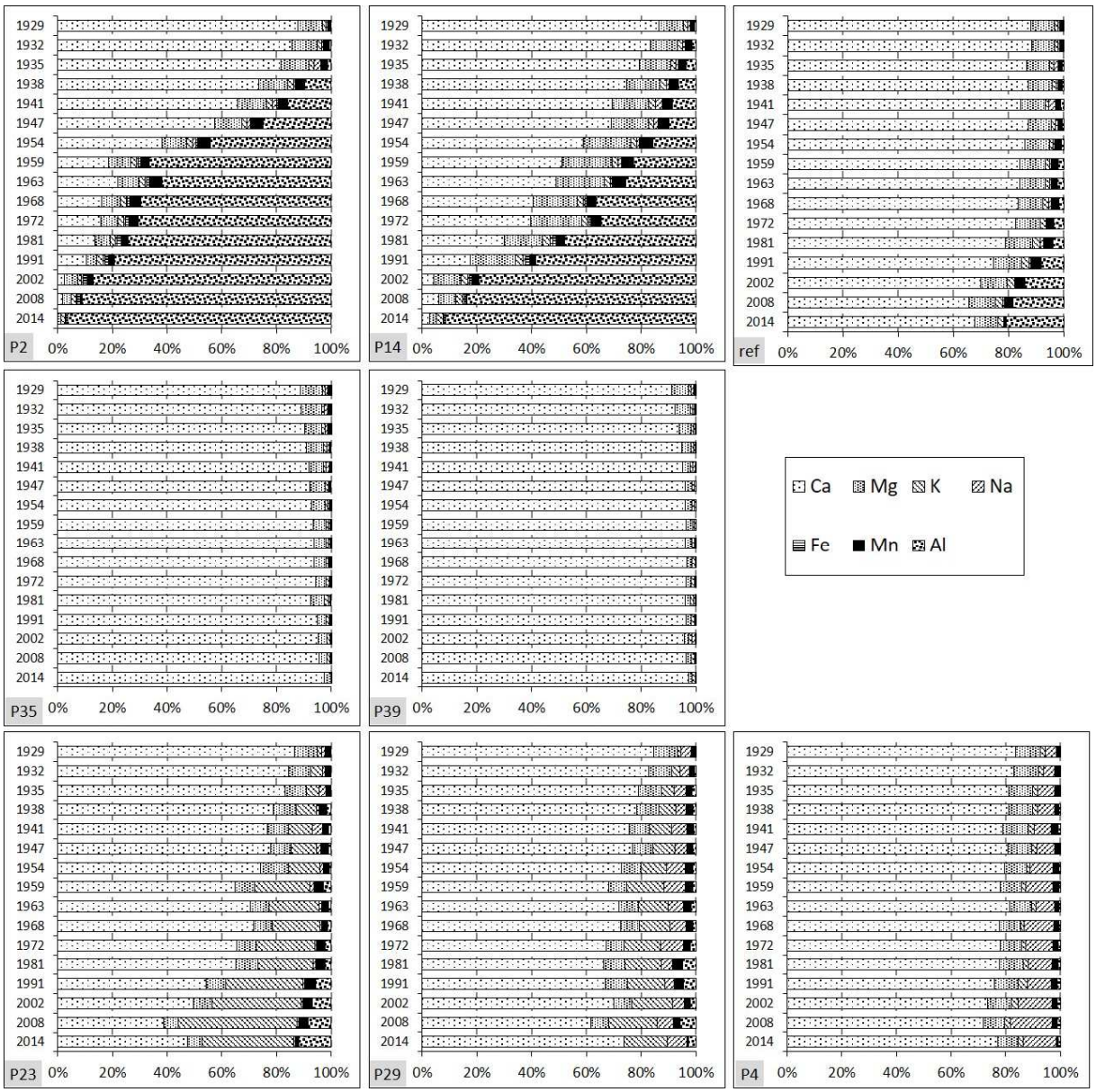
1929
1932
1935
1938
1941
1947
1954
1959
1963
1968
1972
1981
1991
2002
2008
2014
P2
P14
ref
P35
P39
P23
P29
P4
0%
20%
40%
60%
80%
100%
Ca
Mg
K
Na
Fe
Mn
Al

2

3 Fig. 4.

4

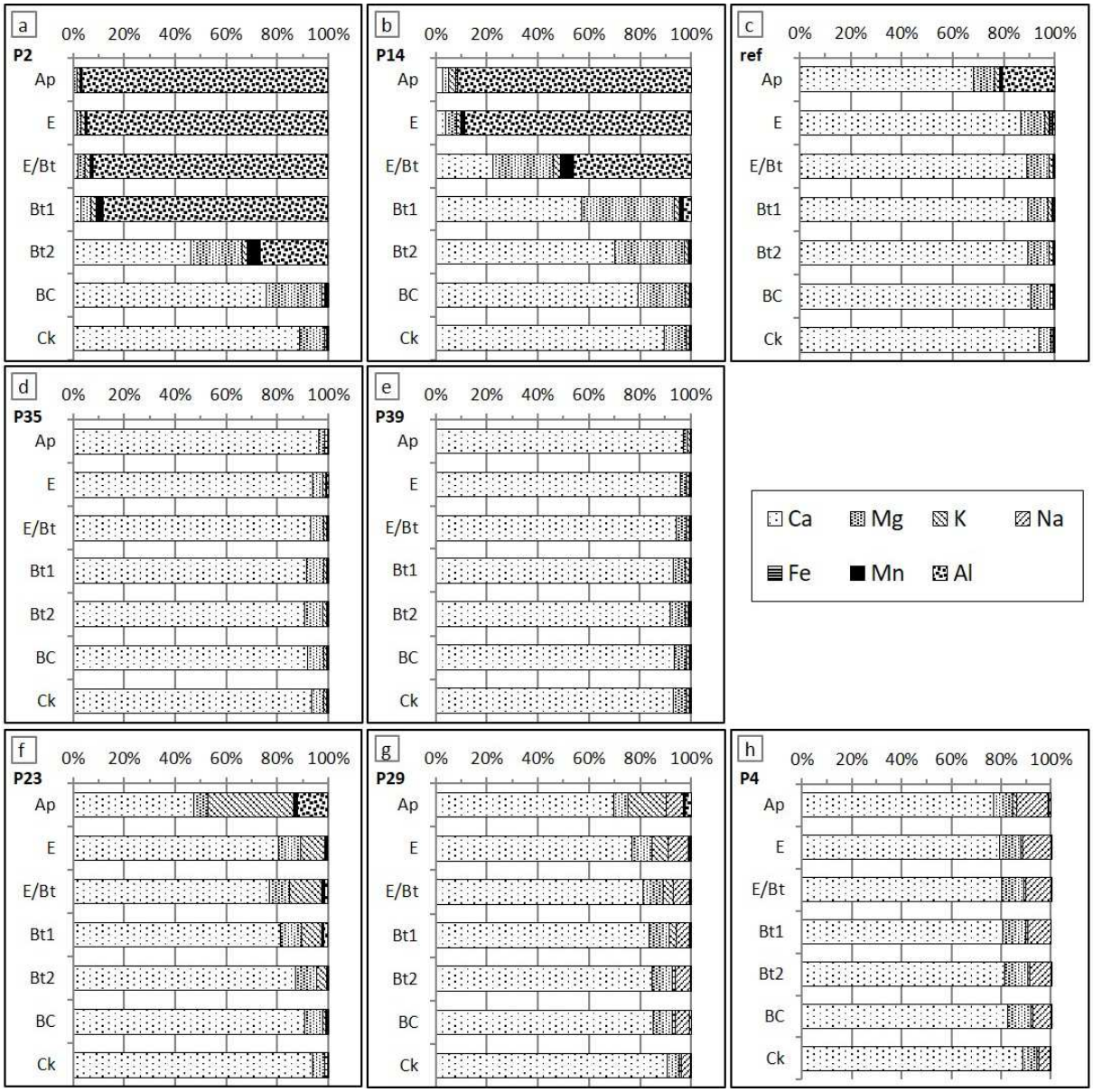
a
P2
b
P14
c
ref
d
P35
e
P39
f
P23
g
P29
h
P4
0% 20% 40% 60% 80% 100%
Ap
E
E/Bt
Bt1
Bt2
BC
Ck
Ca
Mg
K
Na
Fe
Mn
Al

Fig. 5.

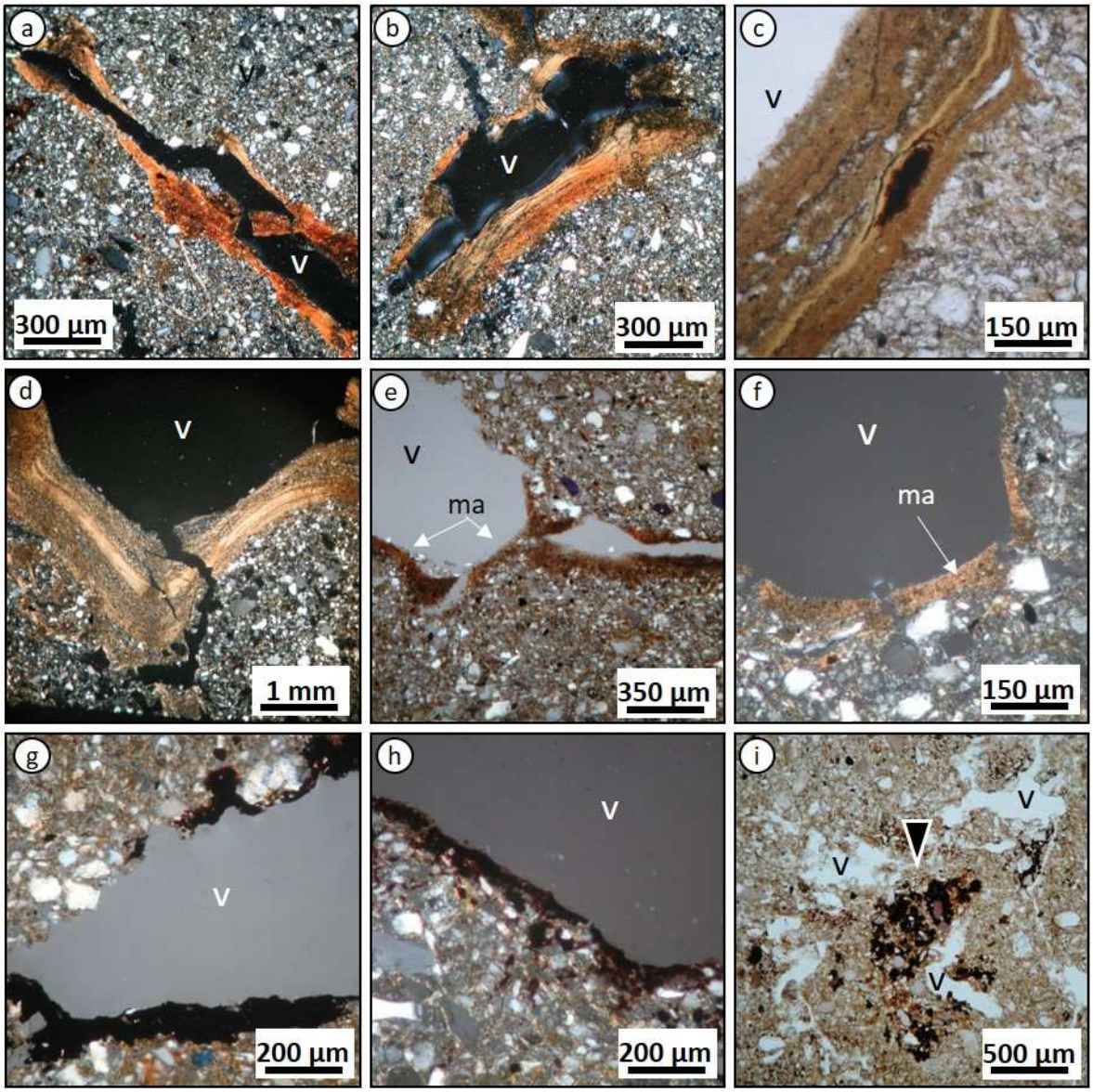
a
V
V
300 µm
b
V
300 µm
c
V
150 µm
d
V
1 mm
e
V
ma
350 µm
f
V
ma
150 µm
g
V
200 µm
h
V
200 µm
i
V
V
V
500 µm

Fig. 6.

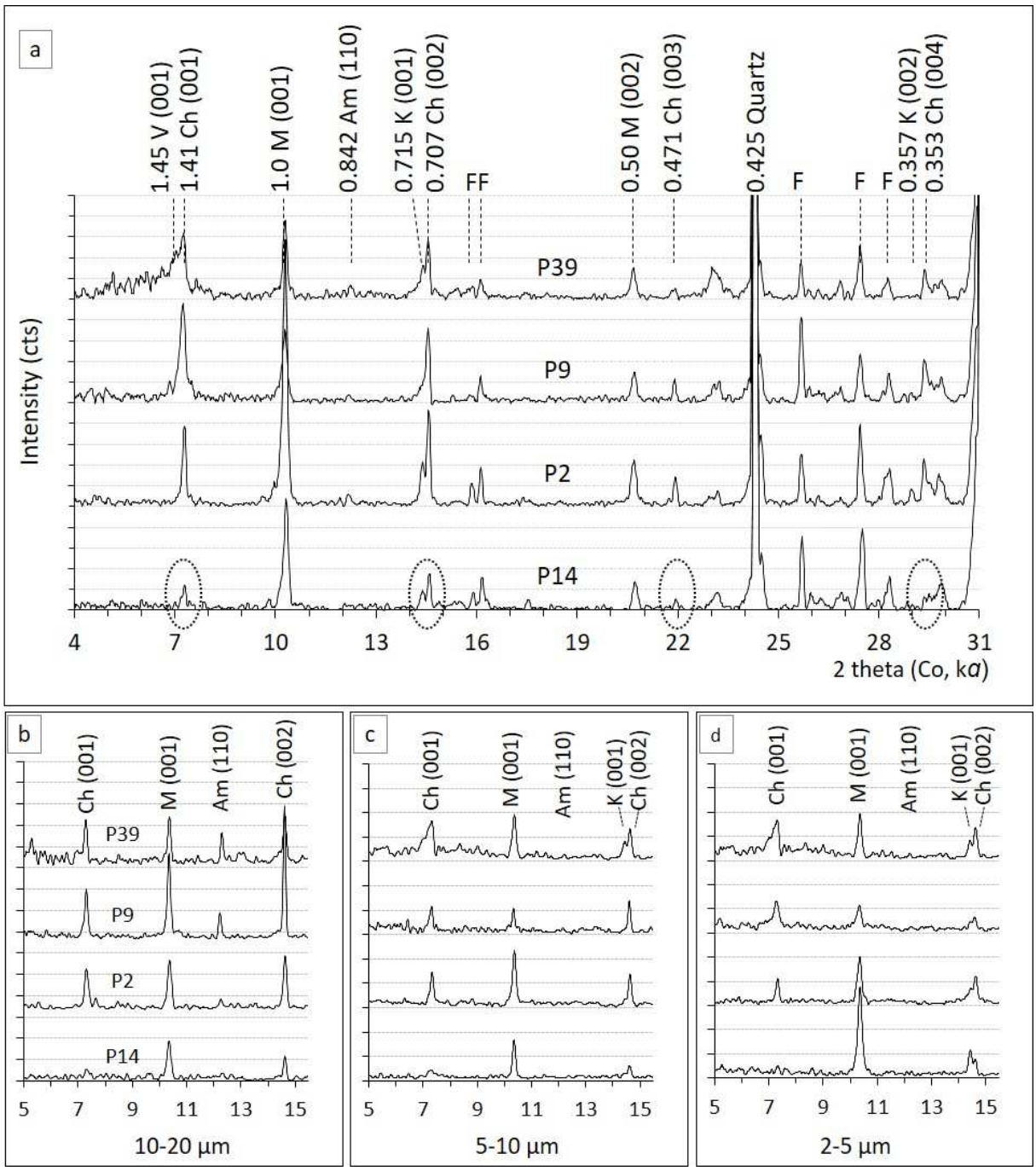
a
1.45 V (001)
1.41 Ch (001)
1.0 M (001)
0.842 Am (110)
0.715 K (001)
0.707 Ch (002)
FF
0.50 M (002)
0.471 Ch (003)
0.425 Quartz
F
F
F
0.357 K (002)
0.353 Ch (004)
P39
P9
P2
P14
Intensity (cts)
4
7
10
13
16
19
22
25
28
31
2 theta (Co, kα)
b
Ch (001)
M (001)
Am (110)
Ch (002)
P39
P9
P2
P14
5
7
9
11
13
15
10-20 µm
c
Ch (001)
M (001)
Am (110)
K (001)
Ch (002)
5-10 µm
d
Ch (001)
M (001)
Am (110)
K (001)
Ch (002)
2-5 µm

Fig. 7.

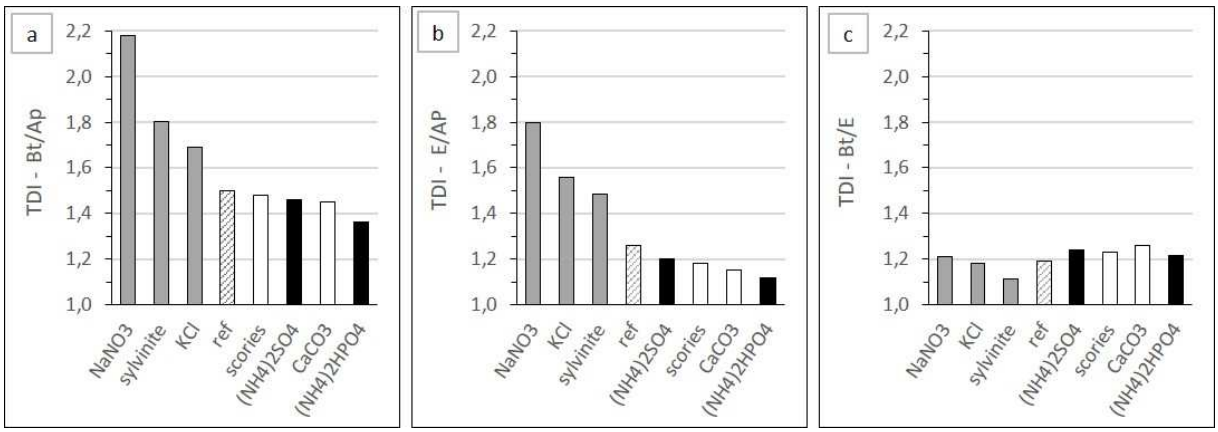
a
TDI - Bt/Ap
2,2
2,0
1,8
1,6
1,4
1,2
1,0
NaNO3
sylvinite
KCl
ref
scories
(NH4)2SO4
CaCO3
(NH4)2HPO4
b
TDI - E/AP
2,2
2,0
1,8
1,6
1,4
1,2
1,0
NaNO3
KCl
sylvinite
ref
(NH4)2SO4
scories
CaCO3
(NH4)2HPO4
c
TDI - Bt/E
2,2
2,0
1,8
1,6
1,4
1,2
1,0
NaNO3
KCl
sylvinite
ref
(NH4)2SO4
scories
CaCO3
(NH4)2HPO4

Fig. 8.

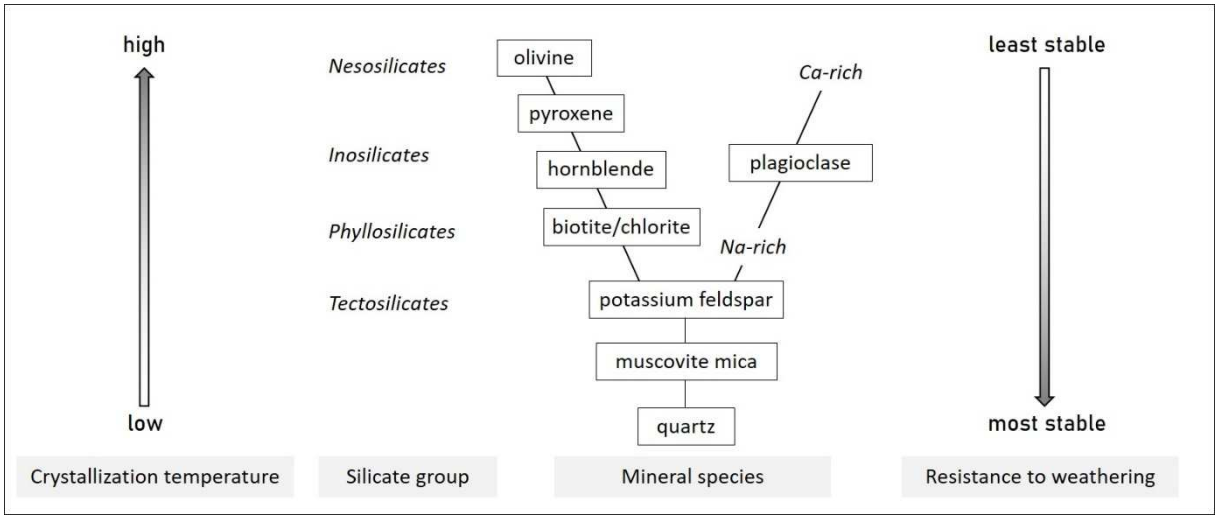
high
low
Crystallization temperature
Nesosilicates
Inosilicates
Phyllosilicates
Tectosilicates
Silicate group
olivine
pyroxene
hornblende
biotite/chlorite
potassium feldspar
muscovite mica
quartz
Ca-rich
plagioclase
Na-rich
Mineral species
least stable
most stable
Resistance to weathering

Fig. 9.

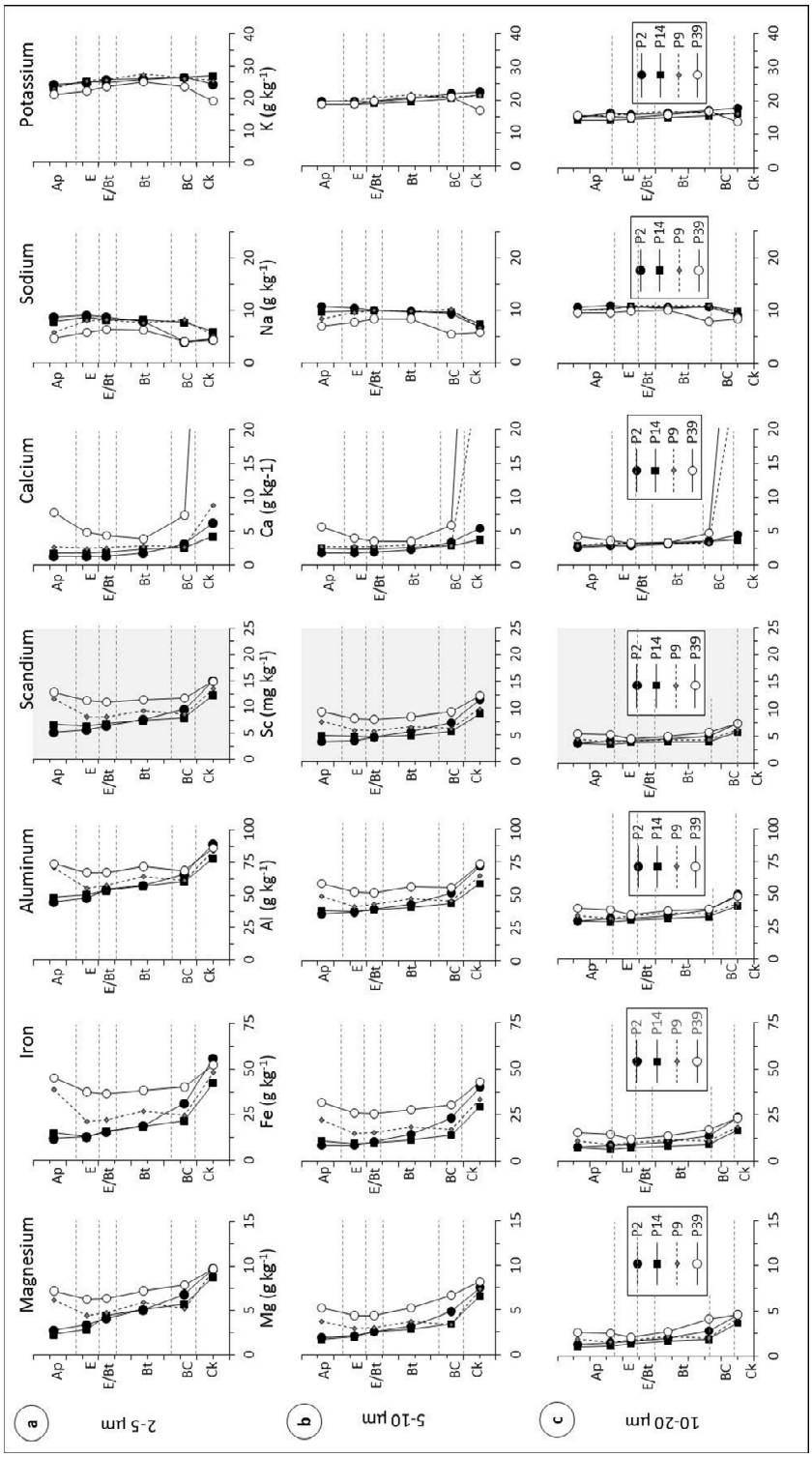
Magnesium
Iron
Aluminum
Scandium
Calcium
Sodium
Potassium
Mg (g kg-1)
Fe (g kg-1)
Al (g kg-1)
Sc (mg kg-1)
Ca (g kg-1)
Na (g kg-1)
K (g kg-1)
Ap
E
E/Bt
Bt
BC
Ck
P2
P14
P9
P39
a
2-5 µm
b
5-10 µm
c
10-20 µm

Fig. 10.

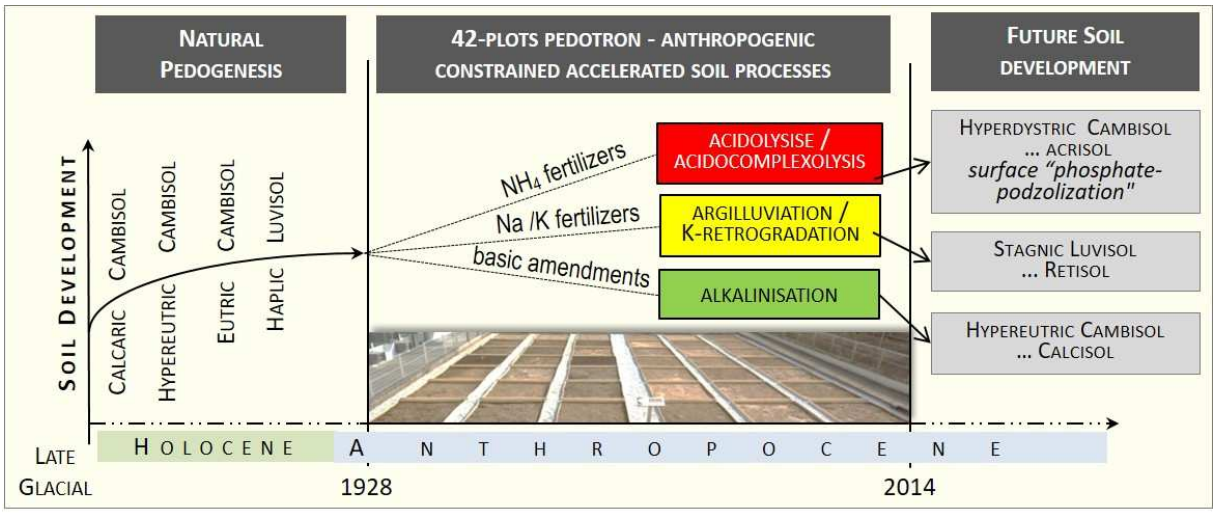
NATURAL PEDOGENESIS
42-PLOTS PEDOTRON - ANTHROPOGENIC CONSTRAINED ACCELERATED SOIL PROCESSES
FUTURE SOIL DEVELOPMENT
SOIL DEVELOPMENT
CALCARIC CAMBISOL
HYPEREUTRIC CAMBISOL
EUTRIC CAMBISOL
HAPLIC LUVISOL
NH4 fertilizers
Na /K fertilizers
basic amendments
ACIDOLYSISE / ACIDOCOMPLEXOLYSIS
ARGILLUVIATION / K-RETROGRADATION
ALKALINISATION
HYPERDYSTRIC CAMBISOL ... ACRISOL
surface "phosphate-podzolization"
STAGNIC LUVISOL ... RETISOL
HYPEREUTRIC CAMBISOL ... CALCISOL
LATE GLACIAL
HOLOCENE
ANTHROPOCENE
1928
2014